S9 Quantum Optics and Nonlinear Optics
Óptica Cuántica y Óptica No Lineal (GEOCONL-GELUR)

13/07 Wednesday afternoon, Aula 1.1 bis

15:30-15:45 Laura Rodríguez Suñé (Univ. Politecnica Catalunya)
Combined experimental-theoretical study of harmonic generation in silicon at nanoscale

15:45-16:00 Carlos Rodríguez Fernández Pousa (Univ. Miguel Hernández)
Incoherent self-loss-modulated Q-switch in Frequency Shifting Loops

16:00-16:15 Shroddha Mukhopadhyay (Univ. Politecnica Catalunya)
Nonlinear conversion efficiency enhancement in gold grating nanostructure

16:15-16:30 Antonio García Blázquez (Univ. Autónoma de Madrid)
Symmetry indicators of second order photocurrent with application to monolayer GaSe from first principles

16:30-16:45 Adolfo Esteban Martín (Univ. de Valencia)
Interferometric Phase Retrieval via Nonlinear Transient Detection Imaging

16:45-17:00 Elena Pinilla Cienfuegos (Univ. Politecnica Valencia)
Optical bistability based on the integration of a molecular nanomaterial in silicon photonics

17:00-18:00 **Posters and Coffee**

18:00-18:15 David Novoa Fernandez (UPV/EHU)
High-quality compression of ultrafast near-UV light in hollow anti-resonant fibres

18:15-18:30 Miguel López Ripa (Univ. Salamanca)
In-line and ultraestable spatiotemporal characterization of constant and time-varying optical vortices

18:30-18:45 Abraham Loredo Trejo (Univ. de Valencia)
Simultaneous tuning of four-wave mixing and polarization modulation instability in microstructured optical fiber

18:45-19:00 Víctor Wilfried Segundo Staels (Univ. Salamanca)
Use of gas-filled multipass cells to generate clean supercontinuum spectra

19:00-19:15 Carlos Damián Rodríguez Fernández (U. Santiago Compostela)
Ionic Liquids as tunable nonlinear optical materials

19:15-19:30 Luis Sánchez-Tejerina San José (Univ. Salamanca)
"Non-linear, purely magnetic magnetization response to femtosecond structured laser pulses

Posters:

13 Luis Alberto Sánchez Domínguez (Univ. de Valencia)
Novel Methods for the Characterization of Forward Brillouin Scattering in Optical Fibers and its Applications

14 Ignacio López Quintás (Univ. Salamanca)
Collinear optical vortices with tailored topological charge generated by angular momentum transfer

15 Juan Lizarraga Lallana (Univ. Autónoma de Madrid)
Light polarisation under evanescent coupling in exciton-polariton couplers

16 Francisco Javier Serrano Rodríguez (Univ. Salamanca)
High-performance simulations of high-order harmonic generation based on artificial intelligence

17 José Ramón Salgueiro Piñeiro (Univ. Vigo)
Efficient computation of azimuthal perturbation eigenpairs of vortex solitons

18 Manuel Eduardo Barredo Alamilla (Uiv. Nacional Autónoma de Mexico)
Cherenkov radiation in chiral matter

19 Manuel Valiente (Univ. de La Laguna)
Quantum liquids and droplets with low-energy interactions in one dimension

20 Inmaculada Pérez Pérez (University of Jena)
Fiber-based biphoton spectroscopy

S9 Quantum Optics and Nonlinear Optics
Óptica Cuántica y Óptica No Lineal (GEOCONL-GELUR)

14/07 Thursday afternoon, Aula 1.1 bis

15:30-15:45 Alberto Muñoz de las Heras (IFF CSIC - Univ. Trento)
Anyonic Molecules in Atomic Fractional Quantum Hall Liquids: A Quantitative Probe of Fractional Charge and Anyonic Statistics

15:45-16:00 Ivan Morera Navarro (Univ. Barcelona)
Superexchange liquefaction of strongly correlated lattice dipolar bosons

16:00-16:15 Eduardo Zubizarreta Casalengua (UAM - U. Wolverhampton)
Emitting single and squeezed photons

16:15-16:30 "Miguel Cornelles Soriano (IFISC, Illes Balears)"
Photonic reservoir computing using quantum resources

16:30-16:45 Sergi Terradas Briansó (CSIC- Univ. Zaragoza)
Ultrastrong Waveguide QED with Giant Atoms

16:45-17:00 Abel Rojo Francàs (Univ. Barcelona)
Exact diagonalization correction method for a few-particles trapped in a harmonic potential

17:00-18:00 **Posters and Coffee**

18:00-18:15 Rodrigo Martín Hernández (Univ. Salamanca)
Magnetically-pumped High Harmonic Generation with circularly polarized driving fields

18:15-18:30 Juan Jose Esteve Paredes (Univ. Autónoma de Madrid)
Light-matter interaction from density functional theory with application to attosecond electron dynamics

18:30-18:45 Ana García Cabrera (Univ. Salamanca)
Multi-vortex high-harmonic beams from graphene's anisotropy

18:45-19:00 Raúl García Álvarez (Univ. Politécnica de Madrid)
The shortest focused X-Waves with Orbital Angular Momentum

19:00-19:15 Alba de las Heras (Univ. Salamanca)
Extreme-ultraviolet scalar and vectorial vortices with very high topological charge

19:15-19:30 Iker Gomez Viloria (CFM Donostia)
Prohibited optical trapping regimens unlocked by focused OAM beams

Posters:

1 Luis Alberto Sánchez Domínguez (Univ. de Valencia)
Novel Methods for the Characterization of Forward Brillouin Scattering in Optical Fibers and its Applications

2 Ignacio López Quintás (Univ. Salamanca)
Collinear optical vortices with tailored topological charge generated by angular momentum transfer

3 Juan Lizarraga Lallana (Univ. Autónoma de Madrid)
Light polarisation under evanescent coupling in exciton-polariton couplers

4 Francisco Javier Serrano Rodríguez (Univ. Salamanca)
High-performance simulations of high-order harmonic generation based on artificial intelligence

5 Carlos Rodríguez Fernández Pousa (Univ. Miguel Hernández)
Incoherent self-loss-modulated Q-switch in Frequency Shifting Loops

6 José Ramón Salgueiro Piñeiro (Univ. Vigo)
Efficient computation of azimuthal perturbation eigenpairs of vortex solitons

7 Manuel Eduardo Barredo Alamilla (Uiv. Nacional Autónoma de Mexico)
Cherenkov radiation in chiral matter

8 Manuel Valiente (Univ. de La Laguna)
Quantum liquids and droplets with low-energy interactions in one dimension

9 Inmaculada Pérez Pérez (University of Jena)
Fiber-based biphoton spectroscopy

Two lines of space reserved to include
codes of the symposium and of this communication

Combined experimental-theoretical study of harmonic generation in silicon at nanoscale

L. Rodríguez-Suné[1,*], M. Scalora[2], C. Cojocaru[1], N. Akozbek[3], R. Vilaseca[1], J. Trull[1]

[1]*Universitat Politècnica de Catalunya, Physics Department, Rambla Sant Nebridi 22, 08222 Terrassa, Spain.* [2]*Aviation and Missile Center, US Army CCDC, Redstone Arsenal, Huntsville, Al, United States.*
[3]*US Army Space & Missile Defense Command, Tech Center, Redstone Arsenal, AL 35898, United States.*

*laura.rodriguez.sune@upc.edu

Second and third harmonic generation (SHG and THG) are two nonlinear processes in which when light interacts with a nonlinear material, new frequencies are generated. These processes are typically studied in thick materials with high nonlinearities and under phase matching conditions and low material absorption with the aim of achieving high conversion efficiencies. They are described through the nonlinear polarization, which is usually approximated to the electric dipole contribution described by the second and third order susceptibilities $\chi^{(2)}$ and $\chi^{(3)}$. This approximation starts to fail when the nanoscale is reached: SHG and THG conversion efficiencies are drastically reduced and phase matching conditions and absorption no longer play a significant role. In this case, other nonlinear contributions to the nonlinear polarization, such as magnetic dipole and electric quadrupole interactions, must be taken into account.

The development of functional nonlinear silicon photonic devices has advanced significantly in recent years thanks to the progress in nano-fabrication techniques. These devises can emit light, modulate signals electro-optically and process data at speeds higher that electronic chips. Most of the interest in nonlinear silicon photonics is due to its high compatibility with CMOS technology, offering structure sizes down to 10nm at low cost. For this reason, it is crucial to understand how light interacts with semiconductors, such as silicon, at the nanoscale. That is why in this work we present a combined experimental and theoretical study of light matter interaction with nanolayers of silicon with the objective of understanding the intrinsic, nonlinear optical properties of this material at nanoscale. This knowledge can then be used to design structures with more complex topologies.

In Fig.1 we show the experimental set-up we have developed, with which we are capable of measuring harmonic signals from different samples as a function of incident angle, polarization and pump wavelength, and in transmission and reflection. The measurements are compared with numerical results based on a microscopic hydrodynamic model which accounts for different possible contributions to the nonlinear polarization [1,2]. This comparative experimental-theoretical study identifies, distinguishes and explains the different contributions to the harmonics generated by silicon at nanoscale. We measure and estimate the efficiency of the harmonic signal using no assumptions about effective surface or volume nonlinearities other that effective electron masses and densities.

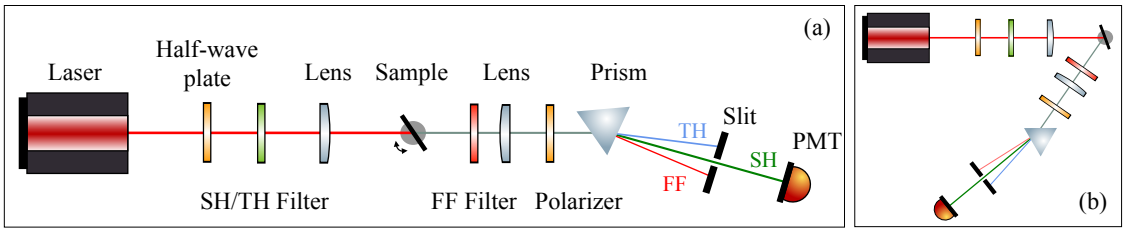

Figure 1. Experimental set-up developed to measure second and third harmonic signals from different samples as a function of pump wavelength, incident angle, polarization and in (a) transmission and (b) reflection.

[1] M. Scalora, M. A. Vincenti, D. de Ceglia, V. Roppo, M. Centini, N. Akozbek and M. J. Bloemer, *Second- and third-harmonic generation in metal-based structures*, Phys. Rev. A 82, 043828 (2010).
[2] L. Rodríguez-Suné, J. Trull, M. Scalora, R. Vilaseca, and C. Cojocaru, *Harmonic generation in the opaque region of GaAs: the role of the surface and magnetic nonlinearities*, Opt. Express 27, 26120-26130 (2019).

Acknowledgements: LRS, JT and CC acknowledge to US Army Research Laboratory Cooperative Agreement Nº W911NF1920279 issued by US ARMY ACC-APG-RTP and Spanish Agencia Estatal de Investigación (project no. PID2019-105089GB-I00/AEI/10.13039501100011033).

Two lines of space reserved to include
codes of the symposium and of this communication

Nonlinear conversion efficiency enhancement in gold grating nanostructure

S. Mukhopadhyay[1,*], J. Trull[1], L. Rodríguez-Suné[1], M. Scalora[2], M. A. Vincenti[3], G. Leo[4], and C. Cojocaru[1]

[1]*Universitat Politècnica de Catalunya, Physics Department, Rambla Sant Nebridi 22, 08222 Terrassa, Spain*
[2]*Aviation and Missile Center, US Army CCDC, Redstone Arsenal, Huntsville, AL, United States*
[3]*Deparment of Information Engineering, University of Brescia, Via Branze 38, 25123 Brescia, Italy*
[4]*Laboratoire Matériaux et Phénomènes Quantiques, Université de Paris & CNRS, 10 rue Alice Domon et Léonie Duquet, 75013 Paris, France*
*e-mail: shroddha.mukhopadhyay@upc.edu

Metal nanostructures are known to exhibit light-matter interaction enhancement under a broad range of irradiation wavelengths by means of plasmonic resonances and have large-scale applications in imaging, sensing, solar cells, surface enhanced spectroscopy etc. Despite their high absorption in the visible and near infrared range, metals are highly nonlinear materials. Resonant metal nanostructures (nanolayers, gratings, nanoantennas or nanoparticles), can largely improve efficiencies of nonlinear optical processes like second and third harmonic generation (SHG and THG) from metal surfaces. At the nanoscale, the conventional approximations used in most of the theoretical models describing the light-matter interactions are not always applicable, so the surface and volume contribution to the nonlinear signal has to be revised [1].

Here we investigate the second and third harmonic generation and enhancement in the opaque region of a gold nano-grating designed to have a resonance at the fundamental wavelength around 800 nm. We present a combined experimental and theoretical approach based on a detailed microscopic hydrodynamic model that relies on temporal and spatial derivatives and accounts for competing surface, magnetic, and bulk nonlinearities arising from both free (conduction) and bound (valence) electrons [2].

We measure the TM and TE components of the SH signal at 400 nm as a function of the fundamental beam polarization, tuning the fundamental wavelength around the resonance and compared with the predictions of out theoretical model. Experimental value of the relative enhancement induced by the grating with respect to SHG from a planar gold nanolayer gives an enhancement factor of 1000 at the central resonant wavelength, perfectly in agreement with the predictions of our model. The same model predicts a 500-enhancement factor for the THG with respect to the plain gold layer.

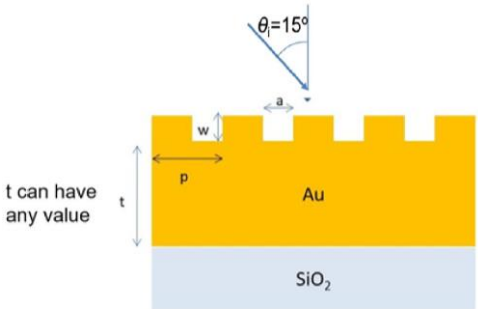

Figure 1. Gold Grating structure; p = 620 nm.

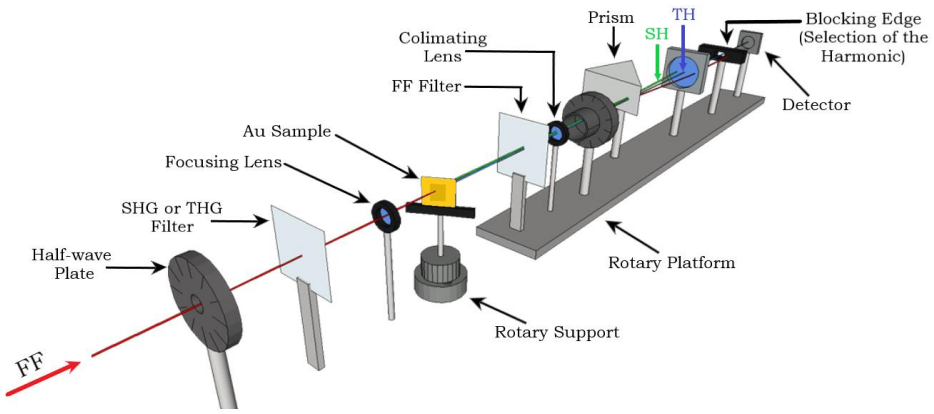

Figure 2. Experimental setup for measurements in transmission

[1] L. Rodriguez-Suñé, J. Trull, C. Cojocaru, et al, *Optics Express* **29**, 8581 (2021).
[2] M. Scalora, M. A. Vincenti, D. de Ceglia, C. Cojocaru, *J. Opt. Soc. Am*, **B 32**, 2129 (2015).

Acknowledgements: SH, LRS, JT and CC acknowledge to US Army Research Laboratory Cooperative Agreement Nº W911NF1920279 issued by US ARMY ACC-APG-RTP and Spanish Agencia Estatal de Investigación (project no. PID2019-105089GB-I00/ AEI/10.13039750110001103 3).

Two lines of space reserved to include
codes of the symposium and of this communication

Symmetry indicators of second order photocurrent & application to monolayer GaSe from first principles

M. A. García-Blázquez[1,*], J. J. Esteve-Paredes[1], J. J. Palacios[1,2]

[1] *Departamento de Física de la Materia Condensada, Universidad Autónoma de Madrid, E-28049 Madrid, Spain.* [2] *Instituto Nicolás Cabrera (INC) and Condensed Matter Physics Center (IFIMAC), Universidad Autónoma de Madrid, E-28049 Madrid, Spain.*

*e-mail: manuelantonio.garcia@uam.es

We present a general analysis of the implications of spatial symmetries on the photogalvanic effect in a crystalline solid, based on its space group and the band representations at the relevant points in the Brillouin zone. This second order photocurrent has a strong dependence on the atomic details of the material [1], which enhances the importance of employing selection rules to provide some sort of guidance in the search of candidate solids to exhibit this effect. Apart from the well-known need to break inversion symmetry, we focus on the role of rotational and mirror symmetries in 2D materials, where bands can be divided into two non-interacting sets according to their parity under a horizontal reflection, whenever that symmetry is present in the system. We find that some of these symmetry requirements can situationally be restrictive at frequencies near the band edge, specially in 2D materials, which points to the introduction of symmetry-perturbing strains as a catalyst for stronger second order photocurrents.

These results are particularized for a crystalline single-layer of GaSe, which is a promising non-linear optical semiconductor. We compute the first and second order conductivity tensors via DFT calculations, which are qualitatively described in terms of band representations, and compare the results at low-energy with the analytical results provided by the ***kp***-formalism [2]. Furthermore, we show explicitly how the sums over the Brillouin zone which are required to compute the conductivity tensors can be reduced to sums over the irreducible Brillouin zone, thereby reducing computation time by a factor of the order of the crystallographic point group of the material.

[1] Ibañez-Azpiroz, J., Tsirkin, S. S., Souza, I. *Physical Review B*, **97(24)**, 245143 (2018).
[2] Cook, A. M., M Fregoso, B., De Juan, F., Coh, S., Moore, J. E. *Nature communications*, **8**(1), 1-9 (2017).

Two lines of space reserved to include
codes of the symposium and of this communication

Interferometric Phase Retrieval via Nonlinear Transient Detection Imaging

A. Esteban-Martín*, J. García-Monreal, E. Roldán, F. Silva, G. J. de Valcárcel

Departament d'Òptica i Optometria i Ciències de la Visió, Universitat de València, Dr. Moliner 50, 46100-Burjassot, Spain.

*e-mail: adolfo.esteban@uv.es

A transient detection imaging system (TDI), also known as optical novelty filter, is an adaptive interferometric device that detects temporal changes in a scene while suppressing its static parts. Removal of background improves contrast and helps visualizing and measuring intensity and phase. Following the first TDI proposal by Cudney et al. [1], most TDI systems are based on photorefractive two-wave mixing [2]. Previous works rely on conventional intensity measurements, where partial information about input signal phase changes are obtained by previous calibration.

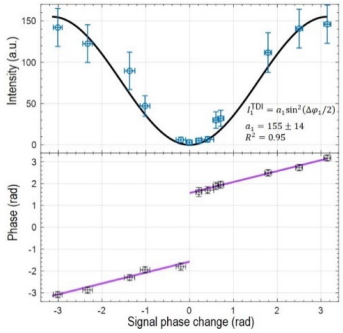

Figure 1. Transient output intensity(top) and phase (bottom) depending on the applied signal-phase change. Intensity is fitted whereas phase follows the linear theoretical Equation.

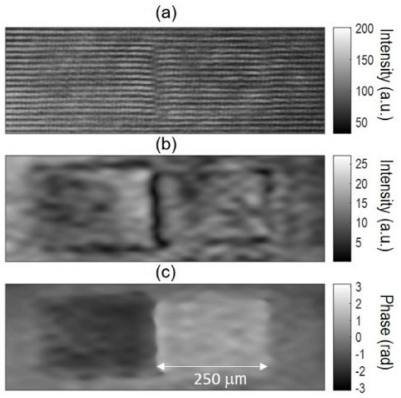

Figure 2. Example of transient interferogram (a), intensity (b) and retrieved differential phase (c) of a squared-shape phase moving object from left to right.

In this work, we report our results on the TDI output complex-field and its relation with the input signal phase changes. The experimental setup is based on a single-frequency laser emitting at 532nm and SBN and BaTiO3 crystals. The laser beam is split into a signal beam, a pump beam, and a reference beam for interferometry. Signal and pump beams intersect at the nonlinear crystal, which has its c^+-axis oriented to get strong energy transfer from signal to pump under steady-state operation. Therefore, the output beam contains images only when the input signal beam changes. The input signal beam is reflected onto a piezo-mirror which allows fine control of phase changes. Output signal phase is retrieved from off-axis holographic Fourier technique which, compared to conventional intensity-based TDI, provides important additional features such as directionality of the phase change, higher resolution, and differential-phase measurement for enhanced sensitivity without calibration.

We have evidenced the linear relation between input and output phases for the entire range from $-\pi$ to π (see Figure 1) in excellent agreement with our theory [3], where the output-signal transient phase, is given by:

$$\frac{\Delta\varphi_1}{2} + \frac{\pi}{2}\operatorname{sign}\Delta\varphi_1$$

and just depends on the input signal phase change $\Delta\varphi_1$, and predicts a π jump "amplification" around zero.

The results indicate that interferometric transient phase measurements improves inference from intensity, reaching $\lambda/30$ resolution (see Figure 1), and provides differential-phase detection. Moreover, we report new results on interferometric transient phase retrieval microscopy of moving objects (see Figure 2).

We believe that this work takes advantage of background suppression with high phase-sign sensitivity, especially important for low-power small-phase change signals sensors, and opens up new possibilities.

[1] R. S. Cudney, R. M. Pierce, and J. Feinberg, *Nature* **332**(6163), 424 (1988).
[2] M. Woerdemann, F. Holtmann, and C. Denz, *Appl. Phys. Lett.* **93**, 021108 (2008).
[3] A. Esteban-Martín, J. García-Monreal, F. Silva, and G. J. de Valcárcel, *Optics Express* **28**, 28782 (2020).

Acknowledgements: We acknowledge financial support from the Spanish Government and EU-FEDER through project PID2020-120056GB-C22.

Two lines of space reserved to include
codes of the symposium and of this communication

Optical bistability based on the integration of a molecular nanomaterial in silicon photonics

Elena Pinilla-Cienfuegos[1,*], Alba Vicente[1], Jorge Parra[1], Juan Navarro Arenas[1], Pablo Sanchis-Kilders[1], Roger Sanchis-Gual[2], Ramon Torres-Cavanillas[2], Mónica Giménez-Marqués[2], Eugenio Coronado[2]

[1]*Nanophotonics Technology Center (NTC), Universidad Politécnica de Valencia, Valencia, Spain.*
[2]*Instituto de Ciencia Molecular (ICMol), Universitat de València, Valencia, Spain.*

*e-mail: epinilla@ntc.upv.es

Electro-optical bistability is a functionality which can be crucial for a wide range of applications as it can enable non-volatile and ultra-low power switching performance [1]. In this work an advance in Nanophotonics is presented with a new approach for the development of low-power on-chip optical switching devices. This new approach is based on the integration of an encapsulated molecular nanomaterial that presents bistable Spin Crossover (SCO) phenomenon at room temperature (RT) in the Si platform [2].

SCO is a spin-state switching phenomenon present in some molecular compounds such as the coordination complexes of transition-metal ions in which, under certain external stimulus (variation of temperature, pressure, electric field, or light irradiation), the electronic configuration can be switched between two molecular spin states, Low Spin (LS) and High Spin (HS) states [3]. Furthermore, the spin state change is accompanied by a change in the structural, magnetic, and optical properties, as well as in the electrical conductivity and color. These properties vary as a function of the external stimulus following a hysteretic response, recognized as one of the most promising aspects of the system since hysteresis confers bistability and thus a memory effect (Figure 1a).

Finally, the SCO material can be synthetized as nanoparticles so that it can be easily integrated in the silicon platform and have the potential to allow optical switching at room temperature (Figure 1b).

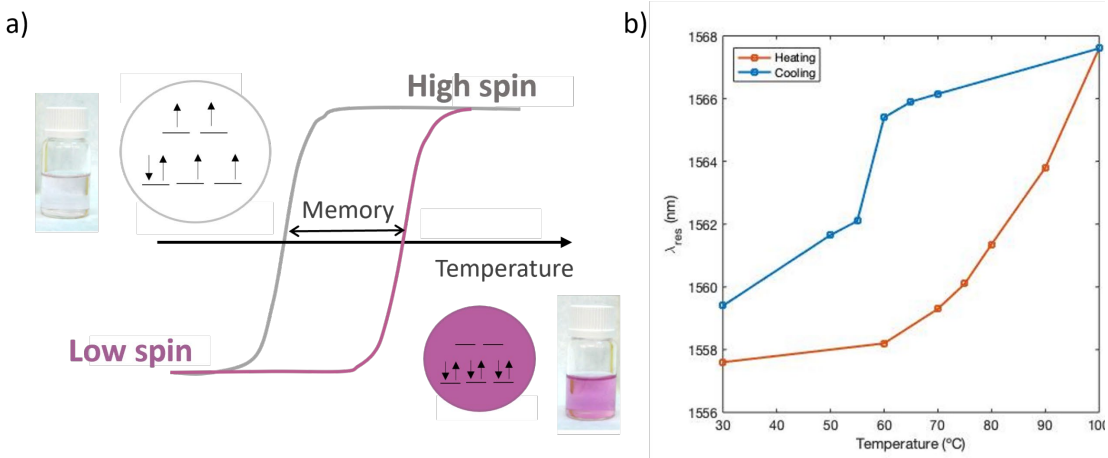

Figure 1. (a) Schematic of the spin configurations and typical spin transition curve with abrupt hysteresis. In the low spin state (LS), electrons are paired, the color of the complex is purple/pink, and the volume is smaller. In the high spin state (HS), the electrons are unpaired, the complex gets a transparent color and the volume increases. (b) Measurement of the optical signal (λ_{res}, resonance frequency) as a function of the temperature where the expected hysterical response is clearly observed. Patent pending (P202130999).

[1] A. H. Atabaki *et al., Nature* **556** (no. 7701), 349 (2018).
[2] M. Giménez-Marqués *et al. J. Mater. Chem. C* **3** (no. 30) 7946 (2015).
[3] O. Kahn and C. Jay Martinez, *Science* **279** (no. 5347) 44 (1998).

Acknowledgements: E.P.-C. gratefully acknowledges support from Generalitat Valenciana (Grant No. SEJIGENT/2021/039).

Two lines of space reserved to include
codes of the symposium and of this communication

High-quality compression of ultrafast near-UV light in hollow anti-resonant fibres

David Novoa[1,2,3,*], Jie Luan[3], Philip St. J. Russell[3]

[1]*Department of Communications Engineering, University of the Basque Country (UPV/EHU), Torres Quevedo 1, 48013 Bilbao, Spain.* [2]*IKERBASQUE, Basque Foundation for Science, Plaza Euskadi 5, 48009 Bilbao, Spain.*
[3]*Max-Planck Institute for the Science of Light, Staudtstrasse 2, 91058 Erlangen, Germany.*

*e-mail: david.novoa@ehu.eus

Coherent ultrafast light sources emitting in the ultraviolet (UV) are important in many fields such as time-resolved spectroscopy [1]. Among the different approaches available for generating ultrashort UV pulses with durations ≲10 fs, broadband-guiding anti-resonant fibres (ARFs) filled with gases stand out owing to their excellent UV transparency and pressure-tunable dispersion [2]. This has permitted, for instance, the compression of near-UV pulses in ambient air-filled ARF [3], but at the expense of spectral red-shifting and limited energy because of the Raman effect originated in the molecular air constituents.

Here we report the generation and direct characterization of μJ-level, ~8.5 fs near-UV pulses centered at 400 nm in an argon-filled ARF. The quality of the pulses Q, defined as the ratio between the pulse energy contained within the main temporal lobe of the pulse to the whole pulse energy (given in percentage), reaches extremely high values up to 98%. This is possible by a judicious choice of fibre parameters (namely length, core size, core-wall thickness, and filling gas pressure) and post-compensation of the spectral phase distortion introduced by the output window of the gas cell and the air path using a combination of dispersive mirrors and glass wedges.

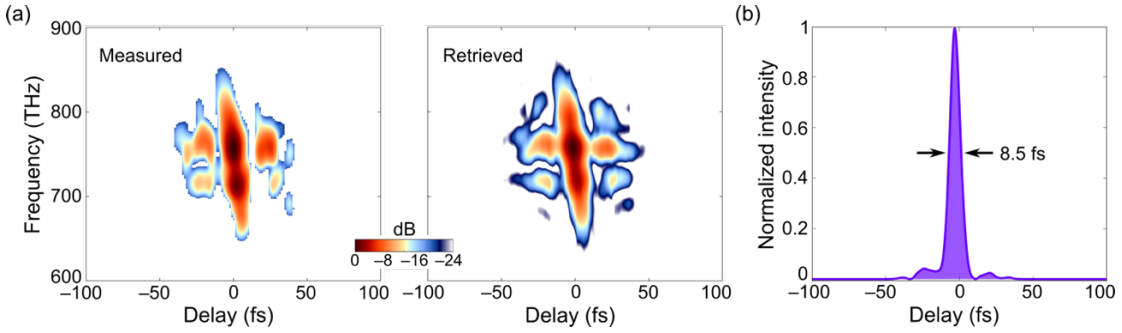

Figure 1. (a) Measured and retrieved spectrograms obtained by self-diffraction frequency-resolved optical gating. Both traces contain the same main features, namely they are composed of a central stripe surrounded by several satellite lobes. (b) Retrieved near-UV pulse with ~8.5 fs duration and Q ~ 98%.

In this study we launched ~60 fs near-UV pulses of 4.4 μJ energy in a 1.15 m-long kagomé-style ARF with ~22 μm-core diameter and ~90 nm core-wall thickness [3]. Upon propagation in the ARF filled with argon at 250 mbar, the pump pulses underwent soliton-effect temporal self-compression, enabled by the interplay of nonlinear self-phase modulation with the negative group-velocity dispersion of the fibre [2]. The outcoupled near-UV pulses were severely distorted in the time domain due to propagation through the MgF_2 window of the output gas cell and the air path to the diagnostics. Following compensation of this excessive positive dispersion using a set of negatively-chirped mirrors and silica wedges, the self-compressed near-UV pulses with μJ-level energy were then characterized using self-diffraction frequency-resolved optical gating. Both measured and retrieved spectrograms (see Fig. 1a) are in very good agreement, yielding a clean pulse of ~8.5 fs duration and extremely high quality as quantified by a Q parameter reaching 98% (Fig. 1b). Interestingly, the near-UV pulses were measured at the point of use, i.e. without need for numerical back-propagation to infer the actual pulse structure at the fibre endface, and therefore may readily find applications in fields such as pump-probe spectroscopy or femtochemistry.

[1] R. Borrego-Varillas *et al.*, *Chem. Sci.* **10**, 9907 (2019).
[2] P. St.J. Russell, P. Hölzer, W. Chang, A. Abdolvand and J. C. Travers, *Nat. Photonics* **8**, 278 (2014).
[3] J. Luan, P. St.J. Russell and D. Novoa, *Opt. Express* **29**, 13787 (2021).

Two lines of space reserved to include
codes of the symposium and of this communication

In-line and ultraestable spatiotemporal characterization of constant and time-varying optical vortices

Miguel López-Ripa*, Íñigo J. Sola, Benjamín Alonso

Departamento Física Aplicada, Universidad de Salamanca, Plaza de la Merced s/n 37008 Salamanca, Spain.

*e-mail: miguellr@usal.es

During the last decades, the generation and study of optical vortices has gained great interest due to their multiple applications such as optical tweezers or optical machining among others [1]. However, the complex set-ups and the high dependency to external perturbations of conventional spatiotemporal characterization techniques [2] complicates their study.

In this contribution, we present the study of constant and time-varying optical vortices using an in-line, robust and ultraestable spatiotemporal characterization technique [3]. The spatiotemporal technique is based on the properties of birefringent uniaxial crystals in order to obtain a bulk lateral shearing interferometer which combines spectral and lateral interferometry. Furthermore, the temporal reference required by our technique is obtained using amplitude swing [4], making the whole system robust against external perturbations. We have taken advantage of the high stability of the whole system, associated with its compact configuration, to characterize temporally and spectrally the wavefronts of optical vortices with constant and time-varying orbital angular momentum (OAM).

The optical vortices were generated using a Ti:Sapphire pulsed laser (central wavelength around 800 nm) and nanostructured plates commonly known as s-waveplates. As explained in [3], depending on the incident beam properties after the s-waveplates we can either generate constant optical vortices or two delayed vortices with an average time-varying OAM. On one hand, in the left part of Fig.1 (Exp. 1) it is shown a snapshot of the spatiospectral characterization of a constant OAM vortex of ℓ=+4, which corresponds to the second harmonic of an optical vortex of ℓ=+2. On the other hand, in the right part of Fig.1 (Exp. 2) they are shown three temporal snapshots of the spatiotemporal characterization of the average structure of two delayed optical vortices with different OAM (ℓ=+2 and ℓ=0). In t_1 and t_3, the individual vortices of ℓ=+2 and ℓ=0 are observed, respectively, whereas t_2 corresponds to its superposition. These results were found to be in good agreement with theoretical simulations [3].

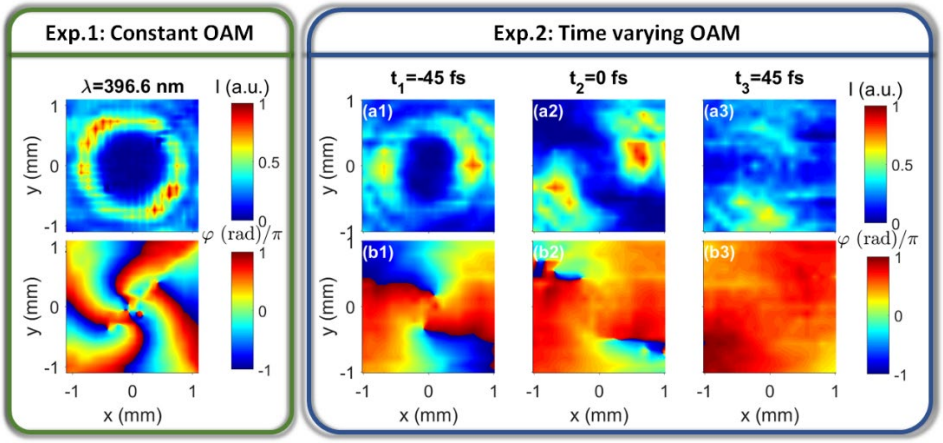

Fig. 1. Green box [Exp. 1]: spatiospectral characterization of a pulsed optical vortex of ℓ=+4. Blue box [Exp. 2]: spatiotemporal characterization of two delayed optical vortices of ℓ=+2 and ℓ=0 for three different times of the pulse.

In conclusion the compact and ultraestable set-up of our spatiotemporal technique enables to easily characterize temporally or spectrally the wavefronts of complex spatiotemporal pulsed beams such as optical vortices. Moreover, the spatiotemporal technique can be used in all the transparency range of the birefringent crystals, so we believe it could be a key tool to ease the characterization of ultrafast phenomena.

[1] Y. Shen, X. Wang, Z. Xie, C. Min, X. Fu, Q. Liu, M. Gong, X. Yuan, *Light Sci. Appl.* **8**, 90 (2019).
[2] S. W. Jolly, O. Gobert, F. Quéré, *J. Opt.* **22**, 103501 (2020).
[3] M. López-Ripa, I. J. Sola, B. Alonso, *Photon. Res.* **10**, 922-931 (2022).
[4] B. Alonso, W. Holgado, I. J. Sola, *Opt. Express* **28**, 15625-15640 (2020).

Two lines of space reserved to include
codes of the symposium and of this communication

Simultaneous tuning of four-wave mixing and polarization modulation instability in microstructured optical fiber

A. Loredo-Trejo[1,2,*], A. Díez[1,2], E. Silvestre[1,3], M. V. Andrés[1,2]

[1]*Laboratory of Fiber Optics, ICMUV, Universidad de Valencia, 46100 Valencia, Spain.* [2]*Departamento de Física Aplicada y Electromagnetismo, Universidad de Valencia, 46100 Valencia, Spain.* [3]*Departamento de Óptica, Universidad de Valencia, 46100 Valencia, Spain.*

*e-mail: abraham.loredo@uv.es

In this communication, we report simple methods to simultaneously generate and tune widely spaced spectral sidebands generated through scalar four-wave mixing (FWM) and polarization modulation instability (PMI) produced in weakly-birefringent microstructured optical fibers (MOFs). In this experimental study, we show that proper control of the fiber properties, in particular, chromatic dispersion and phase birefringence can lead the simultaneous generation and tuning of both nonlinear effects. Changing the refractive index (RI) in the holes surrounding the core of a MOF affects both, chromatic dispersion and birefringence. Thus, tunability of PMI/FWM bands can be attained by fine-tuning the RI in the holes [1, 2]. Here, we used two practical methods. First, a set of solutions of different ethanol-water (EtOH-H_2O) concentrations were prepared and were infiltrated into the fiber. Then, the RI of holes can be adjusted in a wide range by changing the solution concentration. The second method is based on the thermo-optic properties of the liquid infiltrated into the MOFs. In the case of EtOH-H_2O solutions, the thermo-optic coefficient is negative and can be remarkably large for high EtOH concentrations. This second technique enables continuous and dynamic tuning of the RI around an initial value.

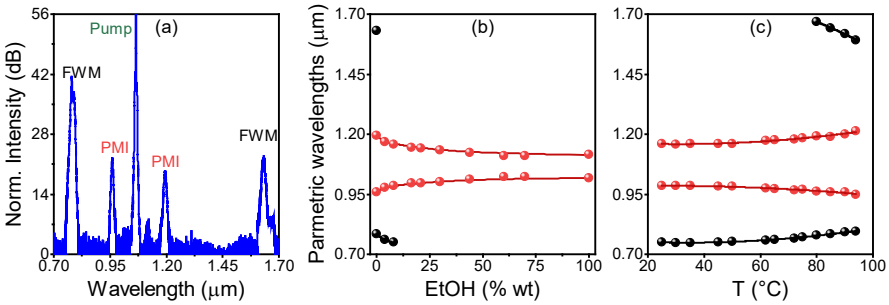

Figure 1. (a) Light spectrum transmitted through the fiber when the fiber holes were filled with a solution at 0 %wt of EtOH. Parametric wavelengths as a function of (b) EtOH concentration and (c) temperature. Pump polarization adjusted to excite the slow-axis eigenmode. PMI and FWM wavelengths are depicted by red and black dots, respectively. Dots are experimental data and lines are a guide to the eye.

We performed the experiments in a liquid-filled, triangular lattice solid-core MOF with hole diameter and pitch of d = 1.8 μm and Λ = 2.9 μm, respectively. We investigate experimentally the simultaneous generation and tuning of PMI/FWM sidebands employing the methods mentioned above. A Nd: YAG microchip laser emitting at 1064 nm was used as the pump. Figure 1(a) shows the light spectrum exiting one fiber, where two pairs of sidebands generated through PMI and FWM can be observed.

Increasing the ethanol concentration of the filling solution causes the FWM sidebands to move away from the pump wavelength, indicating an increase in the frequency shift between the pump and the FWM. The opposite was observed for PMI sidebands, which are shifted towards the pump wavelength, which indicates a decrease of the frequency shift with EtOH concentration. Experiments of PMI/FWM tuning with temperature were performed with the fiber infiltrated with a solution at 8 %wt. Increasing the fiber temperature causes the FWM bands to shift toward the pump wavelength, indicating that the FWM frequency shift decreases with temperature; again, the opposite was observed with the PMI sidebands. We were able to simultaneously tune the PMI and FWM sidebands in the temperature range of the experiments, from 20 °C to 95 °C. Figure 1 (b)-(c) summarizes the parametric wavelengths as a function of EtOH concentrations and temperature.

[1] L. Velázquez-Ibarra, A. Díez, E. Silvestre, and M. V. Andrés, *Optics Letters* **41**, 2600 (2016).
[2] A. Loredo-Trejo, A. Díez, E. Silvestre, and M. V. Andrés, *Optics Letters* **45**, 4891 (2020).

Two lines of space reserved to include
codes of the symposium and of this communication

Use of gas-filled multipass cells to generate clean supercontinuum spectra

V. W. Segundo Staels*, E. Conejero Jarque, J. San Roman

[1]*Grupo de Investigación en Aplicaciones del Láser y Fotónica, Departamento de Física Aplicada, Universidad de Salamanca, E-37008, Salamanca, Spain.*

*e-mail: vwsstaels@usal.es

One of the most efficient nonlinear effects used to achieve ultrashort laser pulses is the self-phase modulation (SPM) [1]. Among the new post-compression setups which have been devised to generate large spectral broadening, multipass cells (MPC) are gaining relevance [2,3]. Multipass cells consist of a cavity formed by two mirrors and usually filled with gas, where a laser pulse travels during multiple roundtrips. To obtain short and clean pulses, one can let the pulse propagate in the enhanced frequency chirp regime, a regime introduced in optical fibers in the 1980s [4]. In this region, the spectrum is broadened with a clean spectral shape and phase because the dynamics is dominated by the nonlinearity, specially by SPM, but with the dispersion being non-negligible.

In order to study if this regime can be achieved in MPCs, we use a 3D numerical to simulate the propagation of a 177 fs full width half maximum (FWHM) Yb laser pulse with a central wavelength of 1030 nm. The propagation occurs along 20 roundtrips in a 40 cm confocal cavity filled with argon. The model calculates the evolution of the envelope of the pulse field affected by diffraction, dispersion, SPM and self-steepening.

We can delimit the enhanced frequency chirp regime by imposing the following three conditions: $L_{NL} < L < L_D$ and $1 < N = \sqrt{L_D/L_{NL}} < 20$, where L is the propagation length, L_{NL} is the nonlinear length and L_D is the dispersion length [5]. The third condition imposes that the maximum peak power reached during the propagation must be below its critical value. In these circumstances, we perform a scan in gas pressure and pulse energy looking for the best conditions of spectrum broadening while conserving a smooth shape.

An optimal region can be found for 10 bar and 100 μJ and its surroundings. In figure 1 we show the result obtained for this particular case. The spectrum obtained (Fig. 1(a)) presents a smooth spectral phase and a clean shape, far from the characteristic SPM oscillations. This shape assures a Fourier Limit compression factor of more than 12, with sidelobes less than 0.4 % of its peak intensity, entering in the few-cycle regime without showing any temporal secondary structure (Fig. 1(b)). This new regime opens a way to obtain clean ultrashort optical pulses using the multipass post-compression scheme

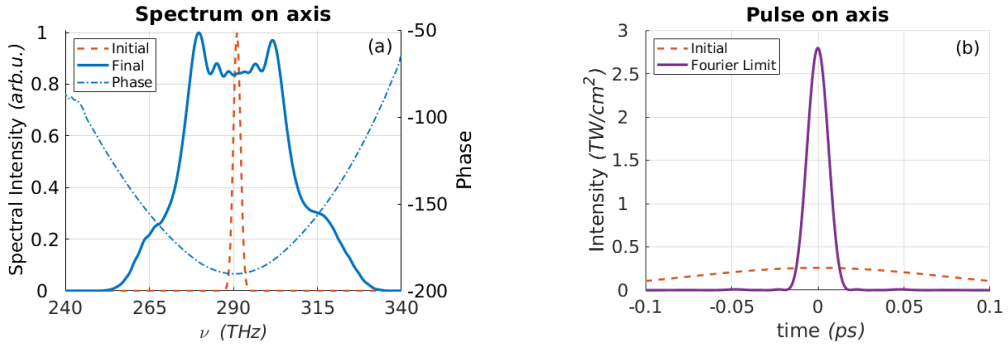

Figure 1. On axis spectral (a) and temporal (b) intensity profiles of a 100 μJ, 177 fs FWHM pulse in confocal cavity filled with 10 bar of argon. Temporal profile is plotted together with the Fourier Limit, reaching a compression factor of more than 12.

[1] T. Nagy, P. Simon, and L. Veisz, *Adv. Phys. X* **6**, 1845795 (2021).
[2] M. Hanna *et al.*, *Laser Photonics Rev.* **15**, 2100220 (2021).
[3] A.-L. Viotti *et al.*, *Optica* **9**, 197 (2022).
[4] W. J. Tomlinson, R. H. Stolen, and C. V. Shank, *JOSA B* **1**, 139 (1984).
[5] A. Couairon and A. Mysyrowicz, *Phys. Rep.* **441**, 47 (2007).

Acknowledgments: Ministerio de Economía y Competitividad (PRE2020-092181); Ministerio de Ciencia e Innovación (PID2019-106910GB-I00).

Ionic Liquids as tunable nonlinear optical materials

Carlos Damián Rodríguez-Fernández[1,*], Luis M. Varela[1], Christian Schröder[2], Raúl de la Fuente, Elena López Lago[1]

[1] *NaFoMat group, Departamento de Física Aplicada and Departamento de Física de Partículas, Universidade de Santiago de Compostela, E-15782 Santiago de Compostela, Spain.* [2] *University of Vienna, Department of Computational Biological Chemistry, Währingerstr. 17, A-1090 Vienna, Austria.*

*e-mail: damian.rodriguez@usc.es

Ionic Liquids (ILs) are a family of ionic materials that are found in the liquid state at temperatures below 100 °C, and, even, at room temperature. Their high thermal and electrochemical stability, negligible vapour pressure and tunability, makes them promising smart materials in different fields. In the case of photonics, ILs exhibit relevant optical properties such as luminescence [1], liquid crystal character [2] or material dispersion [3] that can be task-specifically tuned. In this contribution, we explore, by means of DFT calculations at the B3LYP/6-31++G(d,p) level of theory, the possibility of tailoring the Electro-Optical Kerr Effect (EOKE) susceptibility in ILs throughout designing the extent of charge delocalization in their composing ions. Specifically, we considered the widespread 1-alkyl-3-methylimidazolium cation with alkyl side chains (-CH_2-) of length from one to five units and functionalized derivatives incorporating fluorine atoms (-CF_2-), oxygen atoms (-CH_2-O-CH_2-) or conjugated character (-CH=CH-).

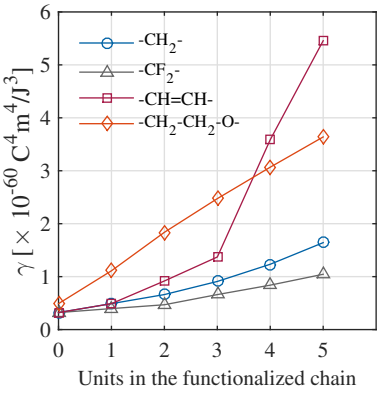

Figure 1. Second hyperpolarizability for the EOKE nonlinear process of different 1-alkyl-3-methylimidazolium based cations differing in the functionalization and length of their side chain.

Our results show that the presence of charge delocalization in the ions has a large impact in their second order hyperpolarizability, γ, and, in general, in their nonlinear optical (NLO) response. Increasing the length of those chains functionalized with saturated units (only σ bonds), produces a moderate increase of the second order hyperpolarizability while, increasing the length of the conjugated chain (that with resonant π bonds), leads to a much higher enhancement of the NLO response. In fact, ILs based on this family of imidazolium cations are able to exhibit EOKE susceptibilities one order of magnitude higher than those of standard KDP, DKDP or BBO nonlinear crystals, suggesting that some ILs could be used as efficient NLO materials.

In conclusion, EOKE susceptibility can be tailored in ILs by means of the smart design of the charge delocalization in their structure and, specially, in the side chains of cationic heterocycles. Our simulations suggest that proper tailoring of the charge delocalization regions can be used to obtain ILs with nonlinear susceptibilities above those of standard nonlinear crystals such as KDP, DKDP or BBO.

[1] K. Tanabe, Y. Suzui, M. Hasegawa, T. Kato, *J. Am. Chem. Soc.* **134**, 5652(2012).
[2] C. Hardacre, J.D. Holbrey, P.B. McCormac, S.E.J. McMath, M. Nieuwenhuyzen, K.R. Seddon, *J. Mater. Chem.* **11**, 346(2001).
[3] C.D. Rodríguez Fernández, Y. Arosa, B. Algnamat, E. López Lago, R. de la Fuente, *Phys. Chem. Chem. Phys.* **22**, 14061(2020).

Acknowledgements: This work was supported by Ministerio de Economia y Competitividad (MINECO) and FEDER 17 Program through the projects (MAT2017-89239-C2-1-P); Xunta de Galicia and FEDER (GRC ED431C 2016/001, ED431D 2017/06, ED431E2018/08). C. D. R. F. thanks the support of Xunta de Galicia through the grant ED481A-2018/032. We also thank the Centro de Supercomputacion de Galicia (CESGA) facility, Santiago de Compostela, Galicia, Spain, for providing the computational resources employed in this work.

Non-linear, purely magnetic magnetization response to femtosecond structured laser pulses

Luis Sánchez-Tejerina[1,*], Rodrigo Martín-Hernández[1], Rocío Yanes[2], Luis Plaja[1], Luis López-Díaz[2], Carlos Hernández-García[1]

[1]*Grupo de Investigación en Aplicaciones del Láser y Fotónica, Dpto. Física Aplicada, Universidad de Salamanca, E-37008, Salamanca, Spain.*
[2]*Dpto. Física Aplicada, Universidad de Salamanca, E-37008, Salamanca, Spain.*

*e-mail: luis.stsj@usal.es

Since the pioneering work on ultrafast laser induced demagnetization [1], femtosecond (fs) laser pulses have attracted a lot of interest as a unique path to achieve sub-ps control of magnetic states. Most of the phenomena involved in these studies are related with non-linear effects of the electric field on the magnetization of the sample [2]. Nonetheless, the recent technological advances in the development of structured laser pulses have opened the possibility to study non-linear effects induced solely by the magnetic field. In particular, the use of azimuthally polarized ultrafast laser pulses. allows for the generation of Tesla-scale fs magnetic fields, isolated from the electric field [3]. Such novel isolation of the magnetic field poses the question of the effect of the magnetic field alone on this ultrashort and ultraintense scale.

In this contribution we show analytically and numerically that isolated circularly polarized magnetic fields promote a non-linear slow cumulative effect on the magnetization of a magnetic sample. Remarkably, such effect scales quadratically with the amplitude of the magnetic field. Our work shows that this effect can be understood as a drift field acting perpendicularly to the plane defined by the circular polarization state, evolving with the envelope of the laser pulse. This effect can be used to obtain purely precessional sub-ps switching with hundreds of Tesla on ferromagnets [4] or even to excite self-sustain oscillations in antiferromagnets with only several tens of Tesla. Our work introduces the possibility to perform ultrafast magnetization from non-linear magnetic effects in which undesirable effects that typically appear from the use intense electric fields, such as heating of the sample, can be avoided.

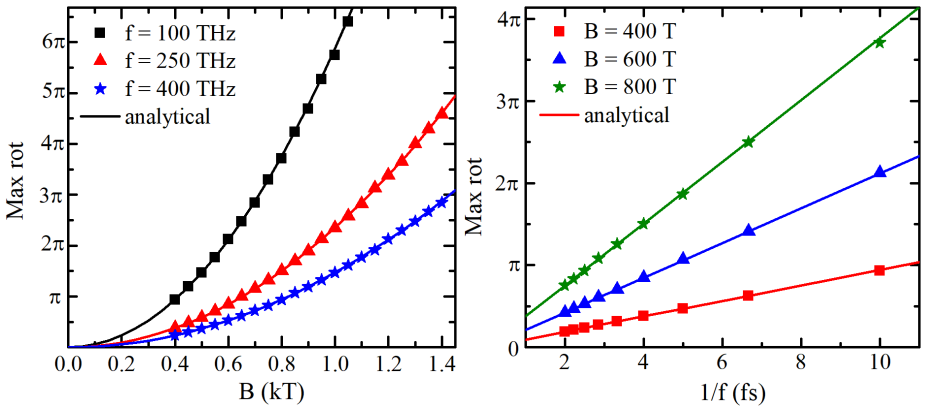

Figure 1. (a) Total rotation of a ferromagnetic sample after the application of a laser pulse of width $t_p = 750$ fs as a function of the magnetic field amplitude. (b) Total rotation of a ferromagnetic sample after the application of a laser pulse of width $t_p = 750$ fs as a function of main frequency.

[1] E. Beaurepaire, J.-C. Merle, A. Daunois, and J.-Y. Bigot, *Phys. Rev. Lett.* **76**, 4250 (1996).
[2] C. Wang, Y. Liu, *Nano Convergence* **7** (2020).
[3] M. Blanco, F. Cambronero, M. T. Flores-Arias, E. Conejero Jarque, L. Plaja, and C. Hernández-García *ACS Photonics* **6** (2019).
[4] L. Sánchez-Tejerina, R. Yanes, R. Martín-Hernández, L. Plaja, L. López-Díaz, C. Hernández-García, *in preparation*.

Acknowledgements: This work has been funded by the ERC Starting Grant ATTOSTRUCTURA, grant agreement No. 851201; Ministerio de Ciencia de Innovación y Universidades (PID2019-106910GB-I00, RYC-2017-22745); Junta de Castilla y León FEDER (SA287P18).

Two lines of space reserved to include
codes of the symposium and of this communication

Anyonic Molecules in Atomic Fractional Quantum Hall Liquids: A Quantitative Probe of Fractional Charge and Anyonic Statistics

Alberto Muñoz de las Heras[1,2,*], Elia Macaluso[2], Iacopo Carusotto[2]

[1]*Institute of Fundamental Physics IFF-CSIC, Calle Serrano 113b, 28006 Madrid, Spain.*
[2]*INO-CNR BEC Center and Università di Trento, via Sommarive 14, 38123 Trento, Italy.*
*e-mail: a.munozdelasheras@gmail.com

Fractional quantum Hall (FQH) liquids are strongly correlated phases of matter arising in strongly interacting two-dimensional systems subjected to an external magnetic field. Such systems host quasihole and quasiparticle excitations known as anyons that feature fractional charge and intermediate statistics that fall outside the traditional distinction between bosons and fermions. Notwithstanding its exotic nature and the promising perspectives that anyons open up for topological quantum computing, a conclusive signature of anyonic statistics has long remained elusive [1]. Here we studied the quantum dynamics of massive impurities embedded in a strongly interacting, two-dimensional atomic gas driven into the FQH regime under the effect of a synthetic magnetic field. For suitable values of the atom-impurity interaction strength, each impurity can capture one or more quasihole excitations of the FQH liquid, forming a bound molecular state with novel physical properties [2,3]. An effective Hamiltonian for such anyonic molecules is derived within the Born-Oppenheimer approximation, which provides renormalized values for their effective mass, charge, and statistics by combining the finite mass of the impurity with the fractional charge and statistics of the quasiholes. The renormalized mass and charge of a single molecule can be extracted from the cyclotron orbit that it describes as a free particle in a magnetic field. The anyonic statistics introduces a statistical phase between the direct and exchange scattering channels of a pair of indistinguishable colliding molecules and can be measured from the angular position of the interference fringes in the differential scattering cross section. Implementations of such schemes beyond cold atomic gases are highlighted, in particular, in photonic systems. Our results were published in [4].

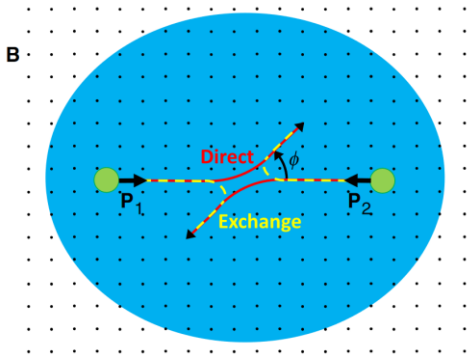

Figure 1. Scattering of two anyonic molecules (green circles) formed by the binding of the same number of quasiholes to a pair of identical impurities in the bulk of a FQH fluid (blue region). The two molecules are given momentum kicks against each other (P1 and P2, respectively). Because of their indistinguishability, two scattering channels contribute to the differential scattering cross section at an angle ϕ: The two channels are labeled as "direct" (red, solid trajectories) and "exchange" (yellow, dashed ones) and involve a relative phase determined by the anyonic statistics. As one can guess from textbook two-slit interference, information about the statistics can be extracted from the global position of the interference fringe pattern.

.

[1] David Tong, *Lectures on the Quantum Hall effect*, arXiv:1606.06687 (2016).
[2] Zhang et al., *Physical Review Letters* **113**, 160404 (2014).
[3] Lundholm and Rougerie, *Physical Review Letters* **116**, 170401 (2016).
[4] Alberto Muñoz de las Heras, Elia Macaluso, and Iacopo Carusotto, *Phyical Review X* **10**, 041058 (2020).

Acknowledgements: European Union H2020-FETFLAG-2018-2020 project "PhoQuS" (No. 820392), Provincia Autonoma di Trento, Q@TN initiative, and Google via the quantum NISQ award.

Superexchange liquefaction of strongly correlated lattice dipolar bosons

Ivan Morera[1,2,3*], Rafał Ołdziejewski[4,5], Grigori E. Astrakharchik[6], Bruno Juliá-Díaz[1,2]

[1] *Departament de Física Quàntica i Astrofísica, Facultat de Física, Universitat de Barcelona, E-08028 Barcelona, Spain.* [2] *Institut de Ciències del Cosmos, Universitat de Barcelona, ICCUB, Martí i Franquès 1, E-08028 Barcelona, Spain.* [3] *Institute for Theoretical Physics, ETH Zurich, 8093 Zurich, Switzerland.* [4] *Max Planck Institute of Quantum Optics, 85748 Garching, Germany.* [5] *Munich Center for Quantum Science and Technology, Schellingstrasse 4, 80799 Munich, Germany.* [6] *Departament de Física, Universitat Politècnica de Catalunya, Campus Nord B4-B5, E-08034 Barcelona, Spain*

*e-mail: imorera@icc.ub.edu

Recently, a new class of ultradilute quantum droplets has been produced in ultracold atomic systems, both in bosonic dipolar systems and in bosonic mixtures. Such quantum droplets are characterized by being self-bound objects similar to the case of water droplets. The main difference is that the equilibrium density can be eight orders of magnitude smaller than in liquid water. Furthermore, the stability of these quantum droplets can be understood from a compensation between mean-field interactions and quantum fluctuations.

In this talk I will present a new type of quantum liquids and droplets which appear in dipolar bosonic systems loaded in one-dimensional optical lattices [1]. These appear in the strongly interacting regime and I will show how their formation can be understood from the appearance of superexchange processes. These processes liquefy the system when being close to the self-bound insulating state (Fig. 1). I will discuss how such lattice quantum liquids can be produced in dipolar bosonic systems which could already be realized in current ultracold atomic laboratories by adding a one-dimensional optical lattice.

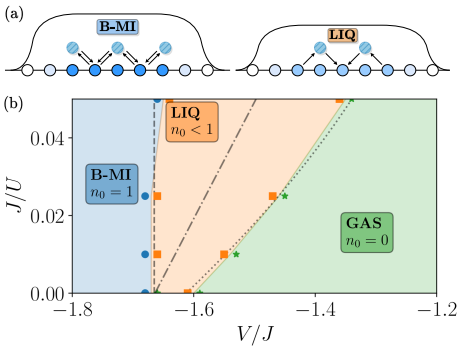

Figure 1. Panel (a): Schematic representation of a density profile in self-bound Mott insulator (B-MI) having unit filling and liquid drop (LIQ) in which particles are bound but holes are present. Arrows indicate the different superexchange processes through doublon formation. Panel (b): Phase diagram for dipolar bosons in a one-dimensional optical lattice. Different phases can be characterized by their respective equilibrium densities n_0. We encounter a gaseous phase (GAS), a liquid one, and a self-bound Mott-insulator. Dashed and dotted-dashed lines denote respectively LIQ-to-B-MI and GAS-to-LIQ transitions obtained in perturbation theory. Dotted line indicates the formation of a bound state (dimer) in the two-body problem.

[1] I. Morera, R. Ołdziejewski, G. E. Astrakharchik, and B. Juliá-Díaz, *arXiv:2204.03906v1* (2022).

Acknowledgements: This work has been funded by Grant No. PID2020-114626GB-I00 from the MICIN/AEI/10.13039 /501100011033 and by the Ministerio de Economia, Industria y Competitividad (MINECO, Spain) under grants No. FIS2017-84114-C2-1-P and No. FIS2017- 87534-P. We acknowledge financial support from Secretaria d'Universitats i Recerca del Departament d'Empresa i Coneixement de la Generalitat de Catalunya, co-funded by the European Union Regional Development Fund within the ERDF Operational Program of Catalunya (project QuantumCat, ref. 001-P001644). R. O. acknowledges support by the Max Planck Society and the Deutsche Forschungsgemeinschaft (DFG, German Research Foundation) under Germany's Excellence Strategy – EXC-2111 – 390814868.

Emitting single and squeezed photons

E. Zubizarreta Casalengua[1,2,*], F. P. Laussy[2,3], E. del Valle[1]

[1] *Departamento de Física Teórica de la Materia Condensada, Universidad Autónoma de Madrid, 28049 Madrid, Spain.* [2] *Faculty of Science and Engineering, University of Wolverhampton, Wulfruna St, Wolverhampton WV1 1LY, UK.* [3] *Russian Quantum Center, Novaya 100, 143025 Skolkovo, Moscow Region, Russia.*

*e-mail: eduardo.zubizarreta@estudiante.uam.es

Many applications of quantum light require the study of photon correlations, which play a central role in Quantum Optics. We show that the statistics of the photons emitted by many light-matter systems, when resonantly excited using coherent sources, can be controlled and optimized at the N-photon level by purposely tuning the excitation, modulating the emission from Sub- to Super-Poissonian due to both external and self-homodyne interferences [1,2]. Particularly, the well-known photon/polariton blockade is investigated in detail, providing a vast and rich landscape of photon correlations and paving the way to subsequent optimization. These works highlight the close relationship between two relevant quantum attributes of light, photon antibunching and quadrature squeezing, which were so far studied as unrelated topics [3]. This interference mechanism can be implemented in photon spectroscopy, where the theory displays interesting results as well. When the laser-qubit detuning is large, a perfect circle of antibunching between photons with different frequencies arises due to quantum interferences, revealing exotic multi-mode squeezing properties of great potential for applications such as quantum spectroscopy and the generation of highly entangled states of light.

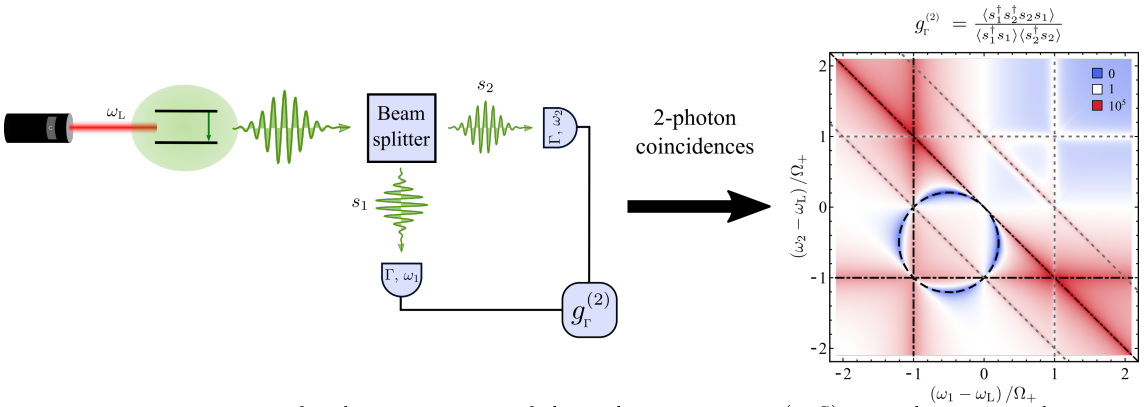

Figure 1. Typical set-up for the measurement of the 2-photon spectrum (2PS), i.e., photon coincidences detected at different frequencies, for a qubit driven by a laser. The 2PS, on the right-hand side, shows a characteristic circle of anticorrelation (in blue), which we have identified as rooted in two-mode squeezing

[1] Conventional and Unconventional Photon Statistics, Zubizarreta Casalengua *et al.*, *Laser & Photonics Reviews* **14**, 1900279 (2020).

[2] Tuning photon statistics with coherent fields, Zubizarreta Casalengua *et al.*, *Phys. Rev. A* **101**, 063824 (2020).

[3] Origin of Antibunching in Resonance Fluorescence, Hanschke *et al.*, *Phys. Rev. Lett.* **125**, 170402 (2020).

Photonic reservoir computing using quantum resources

Jorge García-Beni, Gian Luca Giorgi, **Miguel C. Soriano***, Roberta Zambrini

Instituto de Física Interdisciplinar y Sistemas Complejos (IFISC, UIB-CSIC), Campus Universitat de les Illes Balears E-07122, Palma de Mallorca, Spain.

*e-mail: miguel@ifisc.uib-csic.es

Photonic implementations of brain-inspired computing concepts have achieved state-of-the-art performance in tasks ranging from speech recognition to chaotic time-series prediction. Here, optical feedback is exploited for photonic reservoir computing using quantum resources.

Reservoir Computing is a paradigm of Machine Learning that harnesses the information processing potential of complex dynamical systems [1]. Recently, quantum systems have been suggested as promising candidates for reservoir computing due to the significant growth in phase space degrees of freedom [2]. In this contribution, we propose a photonic platform for reservoir computing and on-line data processing, in the realm of continuous variable quantum optics. A performing reservoir computing scheme requires the availability of a high-dimensionality phase space, a non-linear input-output transformation and a short-term memory, which can be readily available in physical systems [3].

Figure 1 shows a schematic representation of the photonic platform, which includes a feedback loop, nonlinear crystals, an optical beamsplitter and a photodetector. The external input information to be processed is injected in the form of modulated optical pulses. An optical beamsplitter effectively mixes the input pulses with previous pulses that propagate along the feedback loop, providing a mechanism to retain memory into the system. The beamsplitter also allows to send part of the optical pulses to the output photodetector, with the reflectivity of the beamsplitter controlling the memory of the reservoir. The non-linear crystals provide the needed interaction between different optical modes that are contained in the optical pulses. For reservoir computing purposes, we extract the information from the quantum correlations of the optical modes within the pulses, expressed in terms of their covariance matrix.

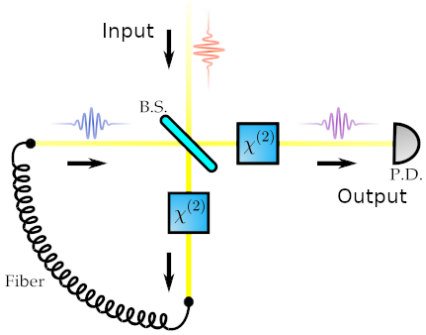

Figure 1. Schematic representation of the proposed photonic platform. The external input to be processed is injected in the form of modulated optical pulses. BS stands for beamsplitter and PD for photodiode. The feedback fiber loop contains a non-linear crystal ($\chi^{(2)}$). The output signal is measured using a homodyne detection scheme.

We tackle the challenge of quantum measurements and back-action in the context of sequential information processing. The performance of the photonic platform, characterized by the information processing capacity [4], is numerically tested for each of the main parameters that can be externally tuned. The role of quantum effects, i.e. squeezing, is addressed in connection with the computational capacity of the system.

Our analytical and numerical results show that, in spite of the dissipative nature of quantum measurements, quantum optical systems can be used for sequential information processing in an experimentally feasible manner and that they may provide advantages over classical dynamical systems.

[1] M. Lukoševičius, and H. Jaeger, *Computer Science Review* **3**, 127–149 (2009).
[2] P. Mujal, R. Martínez-Peña, J. Nokkala, J. García-Beni, G. L. Giorgi, M. C. Soriano, and R. Zambrini, *Advanced Quantum Technologies* **4**, 2100027 (2021).
[3] G. Tanaka, et al., *Neural Networks* **115**, 100–123 (2019).
[4] J. Dambre, D. Verstraeten, B. Schrauwen, and S. Massar, *Scientific Reports* **2**, 514 (2012).

Acknowledgements: We acknowledge the Spanish State Research Agency through the QUARESC project (PID2019-109094GB-C21 and -C22/ AEI / 10.13039/501100011033). We also acknowledge funding by CAIB through the QUAREC project (PRD2018/47).

Ultrastrong waveguide QED with giant atoms

Sergi Terradas-Briansó[1,*],Carlos A. González-Gutiérrez[1],Franco Nori[2,3,4],Luis Martín-Moreno[1], David Zueco[1]

[1] *Instituto de Nanociencia y Materiales de Aragón (INMA), CSIC-Universidad de Zaragoza, Zaragoza 50009, Spain.* [2] *Department of Physics, The University of Michigan, Ann Arbor, Michigan 48109-1040, USA.* [3] *Theoretical Quantum Physics Laboratory, RIKEN Cluster for Pioneering Research, Wako-shi, Saitama 351-0198, Japan.*[4] *RIKEN Center for Quantum Computing (RQC), 2-1 Hirosawa, Wako-shi, Saitama 351-0198, Japan.*

*e-mail: sterradas@unizar.es

The field of waveguide quantum electrodynamics studies the interaction between quantum emitters and propagating one-dimensional electromagnetic fields. One of the more widely used approximations in this field is the dipole approximation, which assumes the emitters can be approximated as point-like particles when compared to the wavelength of the electromagnetic field. In recent years single emitters that break this assumption by coupling to a single electromagnetic mode at different points have been realized experimentally and are known in the literature as giant atoms. These giant atoms have many properties such as tunable decay rates and Lamb shifts, non-Markovian spontaneous emission and bound states due to the interference between the emission from different coupling points and others. See [1] for a recent review.

In the presented work, we extend the theory of giant atoms, previously restricted to perturbative light-matter couplings, to deal with the ultrastrong coupling regime (USC).

Using static and dynamical polaron methods we address the low energy subspace of a giant atom coupled to an ohmic waveguide beyond the standard rotating wave approximation.

We analyze the equilibrium properties of the system by computing the atomic frequency renormalization as a function of the coupling, characterizing the localization-delocalization quantum phase transition for a giant atom, which depends on the spacing between coupling points. We show that virtual photons dressing the ground state are non-exponentially localized around the contact points but instead decay as a power-law as shown in Fig 1.

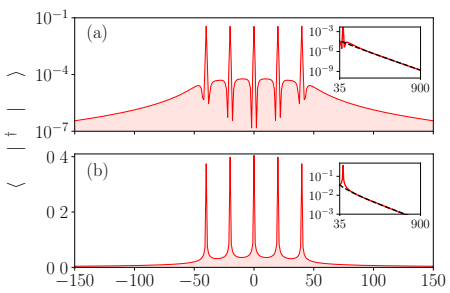

Figure 1. Ground state photons of a giant atom with five equidistant connection points for two coupling strengths α. (a) Illustrates the case is in the delocalized phase, ($\alpha = 1$). (b) Shows a photonic profile in the localized phase ($\alpha = 2$). A power-law fitting is plotted in the insets of both cases.

The spontaneous emission dynamics of an initially excited giant atom are also studied, pointing out the effects of ultrastrong coupling on the Lamb shift and the decay rate, as well as the intrinsic non-Markovianity of the giant atoms. Finally we comment on the existence of the so-called oscillating bound states, for which the emitted radiation is trapped while oscillating between the coupling points of the emitter [2], beyond the rotating wave approximation.

[1] Anton Frisk Kockum, *Quantum Optics with Giant Atoms—the First Five Years. In: International Symposium on Mathematics, Quantum Theory, and Cryptography. Mathematics for Industry, vol 33.*, Springer, Singapore (2021).

[2] Lingzhen Guo, Anton Frisk Kockum, Florian Marquardt and Göran Johansson, *Physical Review Research* **2**, 043014 (2020).

Exact diagonalization correction method for a few-particles trapped in a harmonic potential

Abel Rojo-Francàs[1,2,*], Felipe Isaule[3], Bruno Juliá-Díaz[1,2]

[1] *Departament de Física Quàntica i Astrofísica, Facultat de Física, Universitat de Barcelona, E-08028 Barcelona, Spain.* [2] *Institut de Ciències del Cosmos, Universitat de Barcelona, ICCUB, Martí i Franquès 1, E-08028 Barcelona, Spain.* [3] *School of Physics and Astronomy, University of Glasgow, Glasgow G12 8QQ, United Kingdom.*

*e-mail: abel.rojo@fqa.ub.edu

The study of ultracold atoms is of great interest nowadays due to the great control in laboratories of traps, interactions, number of particles, etc. There are several studies focused on this field [1]. It is frequent to study systems of few particles trapped in a harmonic potential [2] and to consider a contact interaction [3]. One technique used to study this systems is the exact diagonalization [4], whose consists of constructing the Hamiltonian and diagonalizing it exactly. Although, for the harmonic oscillator it is necessary to truncate the basis and as a consequence, the energies obtained are an upper bound of the exact ones.

In our work, we use the fact that the two-particle case has an analytical solution [5] to develop a method to correct the effect of the basis truncation. Solving the two-particle case and introducing a truncation on the basis, we obtain for a given energy, a relation between the value of the exact interaction strength g and the one used in the truncated calculation g' as

$$\frac{1}{g} = \frac{1}{g'} - \frac{1}{g_c}\,, \tag{1}$$

where $1/g_c$ is a correction term with an analytical expression [6]. This value of this correction depends on the state energy and the number of the modes used in the calculation. This correction is exact for the two-particle case even for a small number of modes.

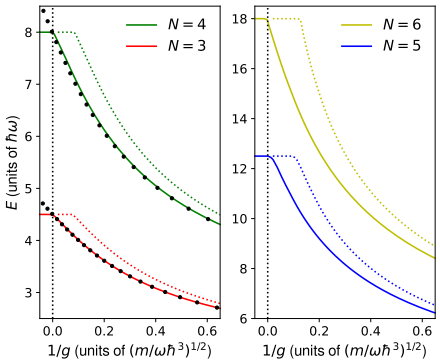

Figura 1: Ground-state energies for $N = 3$ to $N = 6$ distinguishable particles computed using 20 single-particle modes. The dotted lines correspond to the truncated calculations, whereas the solid lines correspond to the corrected energies obtained using Eq. (1). The black circles correspond to the exact values for $N = 3$ and $N = 4$ [3].

We use (1) to correct the energy spectrum for systems with more than two particles. In Fig 1 we show the ground state energy for $N > 2$ as a function of $1/g$. We appreciate the big effect of the correction, especially in the large interacting regime. In addition, for three and four particles, we benchmark our results, with excellent results. For five and six particles, due to the correction, we recover the theoretical energy in the infinite interacting limit.

This method allows a less resource-intensive and more accurate calculation of the energy spectrum using exact diagonalization with a simple additional calculation. Although this method is based on the energy correction, it is also useful for correcting other properties, such as the density profile. In this work, we only consider systems with symmetric interactions: with all interactions equal. Although we suspect that for systems with each interaction different, all of them can be corrected with this procedure for each of their values.

[1] T. Sowiński and M. Á. García-March, *Reports on Progress in Physics* **82**, 104401 (2019).
[2] A. Rojo-Francàs, A. Polls, and B. Juliá-Díaz, *Mathematics* **8**, 1196 (2020).
[3] E. K. Laird, Z.-Y. Shi, M. M. Parish, and J. Levinsen, *Phys. Rev. A* **96**, 032701 (2017).
[4] D. Raventós, T. Graß, M. Lewenstein, and B. Juliá- Díaz, *Journal of Physics B: Atomic, Molecular and Optical Physics* **50**, 113001 (2017).
[5] T. Busch, B.-G. Englert, K. Rzażewski, and M. Wilkens,*Foundations of Physics* **28**, 549 (1998).
[6] A. Rojo-Francàs, F. Isaule, B. Juliá-Díaz arXiv:2202.12749

Acknowledgements: We thank Prof. Joan Martorell for his support in all aspects reported in this work. We also thank Emma Laird for sending us her results for SU(N) fermions from Ref. [3].

Two lines of space reserved to include
codes of the symposium and of this communication

Magnetically-pumped High Harmonic Generation with circularly polarized driving fields

Rodrigo Martín-Hernández*, Luis Plaja, Carlos Hernández-García

[1]*Grupo de Investigación en Aplicaciones del Láser y Fotónica, Departamento de Física Aplicada, Universidad de Salamanca, E-37008, Salamanca, Spain.*

*e-mail: rodrigomh@usal.es

High Harmonic Generation (HHG) is well-stablished as a standard tool to obtain coherent high-frequency light emission and attosecond pulses [1]. In the most common scheme, a linear-polarized electric field interacts with an atomic gas jet generating a fast-oscillating dipole. The process results in the emission of high-order harmonics whose spectrum is characterized by a broad plateau that extends towards a cut-off frequency. On the other side, the simultaneous development of ultrafast structured light beams is opening new scenarios to control strong light-matter interactions. In particular, it has been recently proposed that isolated Tesla-scale femtosecond magnetic fields can arise from azimuthally polarized vector beams [2], enabling alternative perspectives in ultrafast magnetism, spintronics [3], and, why not, in ultrafast, nonlinear, and quantum optics.

In this work, we pioneer a new mechanism in HHG through the use of a circularly polarized electric field simultaneously pumped by a strong, isolated linearly polarized magnetic field. We numerically solve the three-dimensional time-dependent Schrödinger equation in the hydrogen atom. While in the standard HHG scheme the efficient generation of high order harmonics is not feasible with circularly polarized drivers [4], we show that the combined use of intense linearly polarized PHz oscillating magnetic fields not only allows the generation of high-order harmonics, but extends the cut-off frequency by hundreds of harmonic orders (Fig. 1 a). Remarkably, the attosecond pulse associated with the extended spectrum exhibits elliptical polarization with a temporal width of ~80 attoseconds (Fig. 1 b). In this proposal, linearly polarized isolated magnetic fields over 10^4 T are considered, which can be obtained from the use of a stationary wave generated by two counter-propagating laser beams (Fig. 1 c) with intensities around 10^{18} W/cm^2. Such laser beams are easily achieved nowadays in petawatt laser facilities. The stationary wave generates a slab grating in the gas target where the HHG process takes place, therefore diffracting at different angles the generated harmonics. Our work introduces novel HHG schemes aided by petawatt lasers, allowing exotic configurations and the generation of extremely broad high harmonic spectra towards the X-rays.

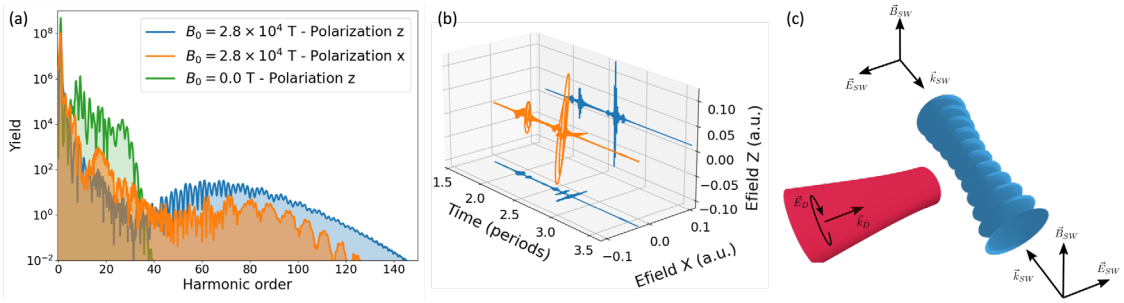

Figure1. (a) HHG spectrum for the standard scheme (linearly polarized driving beam along the z direction) in green, compared with the generated spectrum using the circularly polarized driving beam (in the x-z plane, four-period 800 nm pulse with a peak intensity of $1.6 10^{14}$ W/cm^2) simultaneously pumped with a 800 nm linearly polarized magnetic field of $2.8 10^4$ T (blue and orange stand for the z and x components. (b) Attosecond pulse obtained after filtering the HHG spectrum in (a) above the 60th harmonic order. (c) Scheme of the stationary wave configuration, where the circularly polarized Gaussian driving beam ($\vec{E}_D$) simultaneously pumps HHG with the slabs of magnetic field (blue) arising from the vertically polarized stationary wave ($\vec{B}_{SW}$).

[1] Jeffrey L. Krause, Kenneth J. Schafer, and Kenneth C. Kulander, *Phys. Rev. Lett.,* **68**, 3535 (1992).
[2] M. Blanco, F. Cambronero, M. Teresa Flores-Arias, et al., *ACS Photonics*, **6,** 38 (2019).
[3] Jakob Walowski and Markus Münzenberg; *Journal of Applied Physics,* **120**, 140901 (2016).
[4] K. S. Budil, P. Salières, Anne L'Huillier, T. Ditmire, and M. D. Perry, *Phys. Rev. Lett.,* **48**, 3437 (1993).

Acknowledgements: European Research Council (851201); Ministerio de Ciencia de Innovación y Universidades (PID2019-106910GB-I00, RYC-2017-22745); Junta de Castilla y León FEDER (SA287P18).

Light-matter interaction from density functional theory with application to attosecond electron dynamics

M. Malakhov[1], A. Picón[1], G. Cistaro[1], **J. J. Esteve-Paredes**[2,*], A.J. Uría-Alvarez [2], J.J. Palacios[2,3]

[1] *Departamento de Química, Universidad Autónoma de Madrid, E-28049 Madrid, Spain.*
[2] *Departamento de Física de la Materia Condensada, Universidad Autónoma de Madrid, E-28049 Madrid, Spain.*
[3] *Instituto Nicolás Cabrera (INC) and Condensed Matter Physics Center (IFIMAC), Universidad Autónoma de Madrid, E-28049 Madrid, Spain.*

*e-mail: juan.esteve@uam.es

We present a methodology to address light-matter interaction with focus on attosecond electron dynamics in 2D materials starting from density functional theory calculations. We combine an accurate DFT-based evaluation of optical matrix elements and Berry connections with the time-resolved Schrödinger equation including several laser pulses, both at the infrared and the x-ray regimes. In the end, carrier dynamics and light absorption can be obtained and readily compared with available experiments without the aid of any phenomenological parameters. Our methodology is particularly suited for DFT calculations based on Gaussian basis sets as those used in codes such as GAUSSIAN or CRYSTAL as a post-selfconsistent procedure. The use of Gaussian basis sets saves computational effort, as all coordinate space integrations become analytical. Our procedure also entails a proper quantification of several approximations for optical matrix elements widely used in the literature and its effect in reproducing experimental curves.

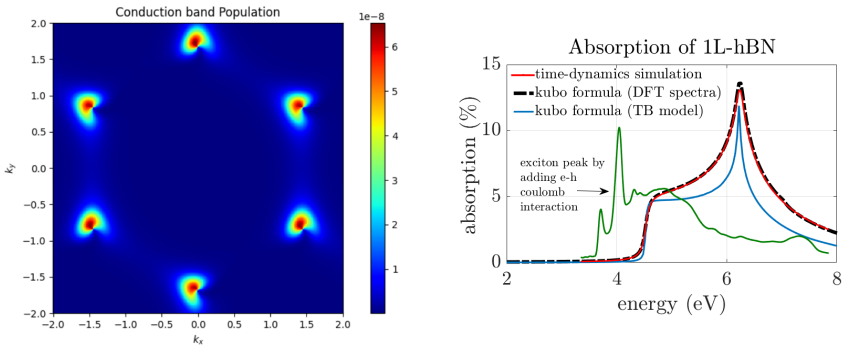

Figure 2. Simulations in monolayer hBN. (Left) Excitation of carriers resolved in reciprocal space. (Right) Light absorption from simulations compared with linear response theory.

[1] G. Cistaro *et al.*, *Phys. Rev. Research* **3**, 013144 (2021).
[2] J.J Esteve *et al.*, arXiv:2201.12290 (2022, submitted).

Two lines of space reserved to include
codes of the symposium and of this communication

Multi-vortex high-harmonic beams from graphene's anisotropy

Ana García-Cabrera*, Roberto Boyero-García, Óscar Zurrón Cifuentes,
Julio San Román, Carlos Hernández-García, Luis Plaja

Departamento de Física Aplicada, Universidad de Salamanca, Plaza de la Merced s/n, E-37008, Salamanca, Spain.

*e-mail: anagarciacabrera@usal.es

High-order harmonic generation (HHG) is a unique tool to produce ultrafast structured laser beams in the extreme ultraviolet (EUV) spectral regime. The deep understanding of this process in gaseous media has triggered the emergence of a wide variety of interaction schemes to control the spatiotemporal properties of the emitted beams, resulting from both spin and orbital angular momentum conservation (SAM and OAM, respectively) [1]. By contrast, HHG in solids has begun to attract the interest of the community more recently. Crystals offer rich scenarios in HHG, where the coupling of the electromagnetic field with the target's structure introduces new phenomena, such as the matter-Talbot effect [2], or the recently observed anisotropic HHG from single-layer graphene [3].

Here, we study HHG in single-layer graphene driven by a mid-infrared vector beam (VB) at normal incidence (see Fig. 1, left panel). The exploration of the coupling of graphene's symmetries with the SAM and OAM of the driving beam requires a macroscopic picture of the interaction. In unstructured media, like gases, HHG preserves the geometry of a cylindrical VB driver [4], which is composed by two OAM modes, $l = \pm 1$. In such case, the simultaneous conservation of SAM and parity leads to the photon composition rules for the qth-order harmonic: $q = n_1 + n_2$ odd and $|n_2 - n_1| = 1$, where $n_1$and n_2 are the number of photons of the two modes. Hence, the OAM of the harmonic beam is restricted to $l = \pm 1$, constituting the cylindrical harmonic VB. In contrast, our theoretical simulations show that graphene's anisotropy [5] imprints two distinct properties into the generated harmonics: (1) a spin-dependent angular diffraction pattern and, (2) high OAM components. Strikingly, the fundamental symmetry associated with the simultaneous spin-orbit conservation forces the splitting of the harmonic beam into a set of EUV vortices with $|l| = 1$ and well-defined helicity. The right panel of Fig. 1 shows the intensity and phase distributions of the multi-vortex formation for the 9th harmonic, for the left circular (a and b) and right circular (c and d) components. Our study highlights the non-trivial interplay between the structural symmetries of the target and the driving beam in HHG, as well as its understanding in terms of both spin-dependent diffraction and the fundamental law of simultaneous conservation of SAM and parity. This opens exciting new routes for the generation of spatially complex EUV structured beams and for a deeper understanding of the ultrafast electron dynamics in solid systems.

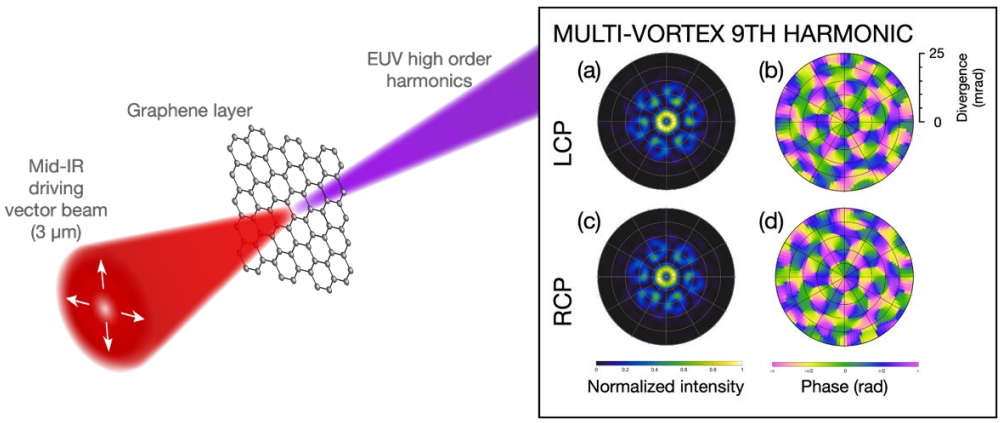

Figure 1. Multi-vortex high-order harmonics in single-layer graphene from a mid-infrared vector beam. The right panel shows the intensity and phase distribution of the 9th harmonic (33 nm).

[1] K. Dorney et al., *Nat. Photonics,* **13**, 123 (2019).
[2] A. García-Cabrera, C. Hernández-García, L. Plaja, *New J. Phys.* **23**, 093011 (2021).
[3] N. Yoshikawa, T. Tamaya, K. Tanaka, *Science* **356**, 736 (2017).
[4] C. Hernández-García et al., I. J. Sola, *Optica* **4**, 520 (2017).
[5] Ó. Zurrón-Cifuentes et al., *Opt. Express* **27**, 7776 (2019).

The shortest focused X-Waves with Orbital Angular Momentum

Raúl García-Álvarez*, Miguel A. Porras

Grupo de Sistemas Complejos, ETSIME, Universidad Politécnica de Madrid, Ríos Rosas 21, 28003 Madrid, España

*e-mail: raul.galvarez@upm.es

In recent years there has been growing interest in ultrashort light pulses with orbital angular momentum (OAM). The first pulses developed with OAM were of Laguerre-Gauss (LG) type. However, these pulsed beams experience diffraction, by which their focus is limited. Therefore, we investigate diffraction-free and dispersion-free wavepackets, the so-called focused X-waves (FX-waves), which also can have OAM. The use of diffraction-free ultrashort pulsed beams would allow for a longer interaction with matter, or long-range transmission of information through OAM channels. In contrast to the more familiar X-waves, FX-waves have recently been synthesized [1] under paraxial and quasi-monochromatic conditions (hundreds of femtoseconds). The future goal would be to shrink these pulses to a few femtoseconds and a nonparaxial, ideally infinitely long focus on the wavelength scale for ultrafast and high-resolution applications.

Here we show the existence of a lower bound to the number of optical cycles for FX-waves carrying OAM similar to that found for X-waves and LG pulses [2,3]. To study the shortest FX-waves with OAM, we have used an ultra-wide spectrum $f(\omega) = e^{-\epsilon\omega}$, with $\epsilon \ll 1$. Given a topological charge m of the vortex carried by the FX-wave, the number of oscillations of the electric field is always larger than $|m|/2$.

The spatiotemporal structure of FX-waves is rather complex. As seen in Fig. 1(a), the different frequencies in the ultra-wide spectrum are spatially distributed at different radii, with the redder frequencies at larger radii, and the whole FX-wave is increasingly blue shifted with m. As a result, the frequency ω_f at the the most intense ring surrounding the vortex, of radius r_M [vertical lines in Fig. 1(a)] is independent of m.

FX-waves containing frequencies from 0 to ∞ are not completely realistic. Therefore, we have studied the effect of truncating the spectrum at a cut-off frequency ω_h, as in Figs. 1 (b) and (c). Since according to Fig. 1(a), higher frequencies are located at smaller radii, truncation would only modify the inner part of the FX-wave. Indeed the radial profiles of fluences, with and without truncation, are almost identical except in the vicinity of the vortex [Fig. 1(b)], and the temporal shapes at the maximum of fluence, r_M [Fig. 1(c)] are identical except for the sidelobes arising from truncation.

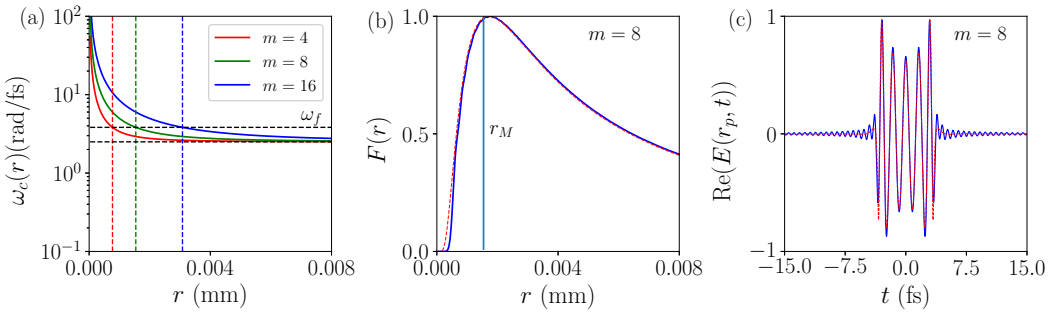

(a) Radial distribution of the central or mean frequency, $\omega_c(r)$, of a FX-wave with superluminal group velocity $v_g = 0.0004$ mm/fs, $\epsilon = 0.2$ fs and $m = 4, 8$, and 16. The vertical lines represent the radii of the most intense ring around the vortex. (b) Radial profile of energy density of a FX-wave with $|m| = 8$ (red dashed line) and with the ultra-wide spectrum upper limited by $\omega_h = 0.7$ rad/fs (solid line). (c) Real electric field at $r = r_M$ of the untruncated and truncated FX-waves in Fig. 1(b). All fields are normalized to their peak values.

[1] Murat Yessenov, Layton A. Hall, et al., arXiv:2201.08297 (2022).
[2] M. A. Porras, *Phys. Rev. Lett.* **122**, 123904 (2019).
[3] M. A. Porras and R. García-Álvarez, *Phys. Rev. A* **105**, 013509 (2022).

Two lines of space reserved to include
codes of the symposium and of this communication

Extreme-ultraviolet scalar and vectorial vortices with very high topological charge

Alba de las Heras[1,*], Alok Kumar Pandey[2], Julio San Román[1], Javier Serrano[1], Luis Plaja[1], Sophie Kazamias[2], Olivier Guilbaud[2], and Carlos Hernández-García[1]

[1]*Grupo de Investigación en Aplicaciones del Láser y Fotónica, Departamento de Física Aplicada, Universidad de Salamanca, Pl. La Merced s/n, Salamanca E-37008, Spain.* [2]*Laboratoire Irène Joliot-Curie, Université Paris-Saclay, UMR CNRS, Rue Ampère, Bâtiment 200, Orsay Cedex F-91898, France.*

*e-mail: albadelasheras@usal.es

Scalar and vectorial vortices are two paradigmatic beam structures carrying orbital angular momentum. On the one hand, a scalar vortex presents a twisted wavefront and homogenous polarization. On the other hand, a vectorial vortex combines a twisted phase and a spatially varying polarization. The topological charge in both scalar and vectorial vortices is the parameter characterizing the number of wavefront twists in one wavelength.

We demonstrate the up-conversion of scalar and vectorial vortices from the infrared (IR) to the extreme-ultraviolet (XUV) regime, by means of the conservation laws in high harmonic generation (HHG). For a scalar vortex, the topological charge in HHG scales linearly with the harmonic order i.e., $\ell_q = q\ell_1$ [1,2]. The analogous conservation law applies for a vector-vortex in terms of the Pancharatnam charge, ie. $\ell_{P,q} = q\ell_{P,1}$ [3]. In Fig. 1, we show the characterization of the 25th harmonic beam resulting from a vortex driver of $\ell_1 = 4$ (left) or from a vector-vortex driver of $\ell_{P,1} = 2$ (right). The experimental XUV beam (top row) is characterized using wavefront sensing metrology, which enables a full measurement of intensity and phase [2]. The theoretical beam (bottom row) is computed in the full quantum strong-field approximation and considers propagation effects in the transverse plane [2,3]. Our results demonstrate the up-conversion of scalar and vectorial phase singularities leading to very high topological charges in the XUV, up to $\ell_{25} = 100$. Such structured XUV beams may encourage advances in high-resolution imaging, attochemistry, or the fundamentals of intense laser-matter interactions.

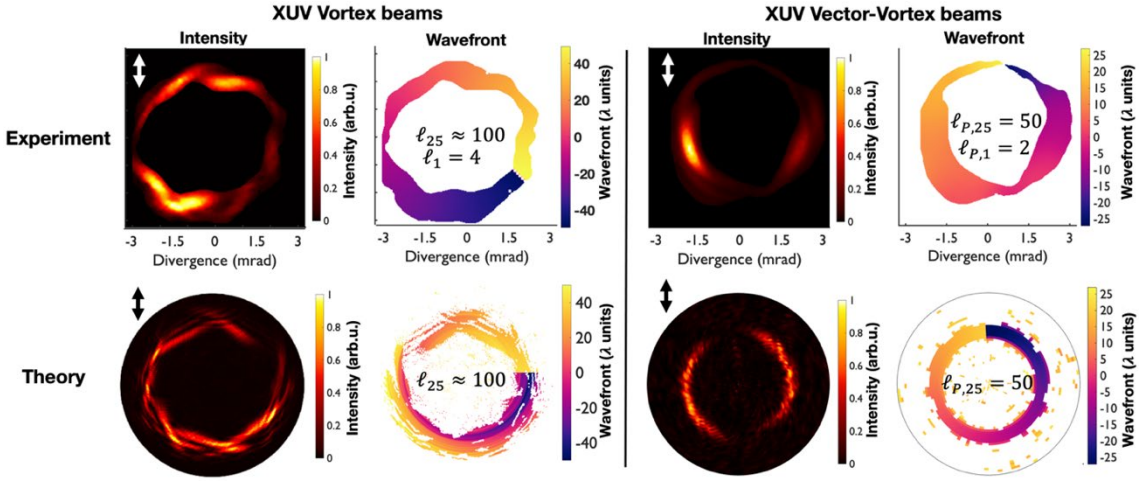

Figure 1. Characterization of XUV vortex and vector-vortex beams. We show the experimental (top row) and theoretical (bottom row) intensity of the vertical polarization projection and wavefront of the 25th harmonic beam. In the left panel, the HHG driver is a vortex of $\ell_1 = 4$, whereas in the right panel the driver is a vectorial vortex of $\ell_{P,1} = 2$.

[1] C. Hernández-García, A. Picón, J. San Román, and L. Plaja, *Phys. Rev. Lett.* **111**, 083602 (2013).
[2] A. K. Pandey, A. de las Heras, T. Larrieu, J. San Román, J. Serrano, L. Plaja, E. Baynard, M. Pittman, G. Dovillaire, S. Kazamias, C. Hernández-García, and O. Guilbaud, *ACS Photonics* **9**, 944 (2022).
[3] A. de las Heras, A. K. Pandey, J. San Román, J. Serrano, E. Baynard, G. Dovillaire, M. Pittman, C. G. Durfee, L. Plaja, S. Kazamias, O. Guilbaud, and C. Hernández-García, *Optica* **9**, 71 (2022).

Acknowledgements: European Research Council (ATTOSTRUCTURA - 851201).

Two lines of space reserved to include
codes of the symposium and of this communication

Prohibited optical trapping regimens unlocked by focused OAM beams

I. Gomez-Viloria[1,*], Á. Nodar[1], M. Molezuelas-Ferreras[1], J. J. M. Varga[1], G. Molina-Terriza[1,2,3]

[1]*Centro de Física de Materiales, Paseo Manuel de Lardizabal 5, 20018 Donostia-San Sebastian, Spain.*
[2]*Donostia International Physics Center, Paseo de Manuel Lardizabal 4, 20018 Donostia-San Sebastián, Spain.*
[3]*IKERBASQUE, Basque Foundation for Science, Maria Diaz de Haro 3, 48013 Bilbao, Spain.*

*e-mail: iker_gomez@hotmail.com

In this work, we present a novel optical trapping method which extends the known trapping regime provided by common focused Gaussian beams, making use of Laguerre-Gaussian (LG) beams with orbital angular momentum (OAM). This new possibility of trapping was discovered thanks to an efficient and general optical forces calculation procedure, formed by a fully analytical formula [1] in terms of well-defined helicity multipoles [2] and which enables displaced laser beams calculations [3,4]. The fields interacting with the sphere were derived by the application of Generalized Lorentz-Mie theory, which gives an analytical description of our system and extends the validity of the calculated expressions to particles of any size. Apart from that, the chosen decomposition provides us some computational tools for increasing the efficiency of the calculated simulations, which at the end of the day, has been crucial in the discovering of the mentioned behaviour. The most remarkable computational technique is the use of "master displacement matrices", which basically multiply chains of these pre-calculated matrices in order to represent any arbitrary displacement of the incident field.

One of our proposals was obtained by the calculation of the stability maps for the Z axis (beam propagation direction) shown in figures 1 and 2. Here is possible to recognize the new zones in the trapping regime unlocked by the use of LG beams with OAM. The totality of the results was fulfilled with stability maps for the X/Y axes, which just confirmed the desired trapping regime.

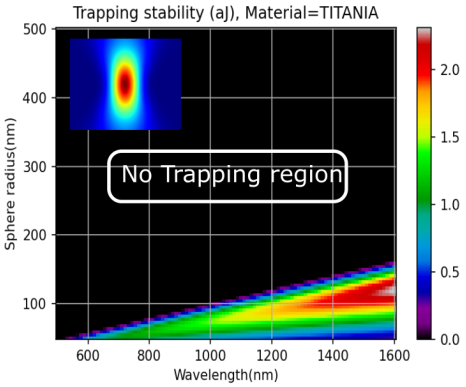

Figure 1. Trapping stability measured as the trapping potential height (aJ). The map has been created for a water suspended Titania (TiO_2) sphere, trapped by Gaussian beam focused with an objective lens of NA=1.20.

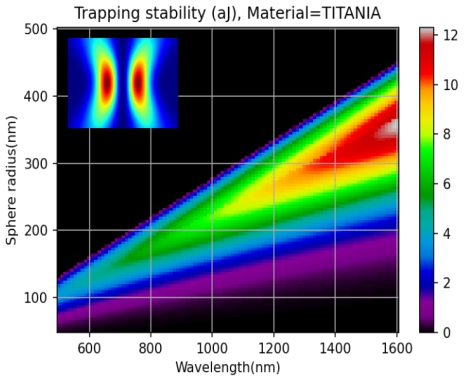

Figure 2. Trapping stability measured as the trapping potential height (aJ). The map has been created for a water suspended Titania (TiO_2) sphere, trapped by LG OAM beam focused with an objective lens of NA=1.20.

On the other hand, due to the well-defined helicity multipole decomposition, our formula naturally distinguish which force terms corresponds to each helicity contained in the incident light beam. In addition, although for the case with spherical particles the calculations are the simplest, it also enables to implement particles with different shapes. This study gives a very useful tool for exploring the relation between optical forces and the angular momentum of light.

[1] A. A. Ranha-Neves and C. Lenz-Cesar, *J. Opt. Soc. Am.* B **36**, 1525 (2019).
[2] M. E. Rose, *Multipole Fields*, Wiley, New York (1955).
[3] X. Zambrana-Puyalto, D. D'Ambrosio, G. Gagliardi, *Laser & Photonics Reviews* **15**, 2000528 (2021).
[4] W.-K. Tung, *Group Theory in Physics*, World Scientific, Singapore (1985).

Two lines of space reserved to include
codes of the symposium and of this communication

Novel Methods for the Characterization of Forward Brillouin Scattering in Optical Fibers and its Applications

L. A. Sánchez[1,*], A. Díez[1,2], J. L. Cruz[1,2] and M. V. Andrés[1,2]

[1]*Laboratory of Fiber Optics, ICMUV, Universidad de Valencia, Dr. Moliner 50, 46100, Burjassot, Spain.*
[2]*Dpto. de Física Aplicada y Electromagnetismo, Universidad de Valencia, Dr. Moliner 50, 46100, Burjassot, Spain.*

*e-mail: luis.sanchez@uv.es

Forward scattering of light by transverse acoustic waves in an optical fiber is an optomechanical phenomenon known as forward Brillouin scattering (FBS). This phenomenon generates frequency shifts in the scattered wave from 30 MHz to 1 GHz in conventional optical fibers. The transverse acoustic mode resonances (TAMRs) behind this phenomenon are the radial $R_{0,m}$ modes and the torsional-radial $TR_{2,m}$ modes, and they can be easily excited in an optical fiber by electrostriction using an optical pump wave [1]. Lately, there has been a growing interest in the development of applications based on FBS such as fiber sensing and also in the use of FBS for fiber characterization.

The detection of the modulation induced by TAMRs in optical fibers is not simple and usually requires hundreds of meters of fiber and using interferometric techniques. Recently, we reported a novel detection technique based on a long-period fiber grating (LPG). The LPG acts as the transducer for the effective index modulation generated by the acoustic wave, converting it into variations in optical transmittance of a probe signal. The LPG allows the detection of the TAMRs with just a few cm of fiber, which reduces the linewidth broadening of the TAMRs due to structural inhomogeneities, obtaining quality factors of up to 5×10^3.

The sensitivity of TAMRs resonance frequency to physical magnitudes as temperature and strain, in conjunction with the LPG interrogation method, allow the development of point sensing schemes based on FBS. In particular, we have demonstrated the combined use of $R_{0,m}$ modes and a subgroup of $TR_{2,m}$ to simultaneously and discriminately measure temperature and strain, thanks to the different response of those acoustic modes to these magnitudes (Figure 1(a)). The accuracies obtained were ± 0.2 °C in the case of temperature and ± 25 με for the strain [2]. The different properties of radial and torsional-radial modes can also be used to characterize the elastic properties of the optical fiber, such as Poisson's ratio. $R_{0,m}$ mode frequencies depend on the longitudinal acoustic velocity of silica, while $TR_{2,m}$ modes depend on the shear acoustic velocity. From an asymptotic fit of the experimental measurements of both types of modes, the ratio between both velocities can be obtained, from which the Poisson's ratio can be calculated [3]. In our experiment we obtained Poisson's ratio of the optical fiber in a temperature range of 100 ºC with a relative error lower than 1 ‰ (Figure 1(b)).

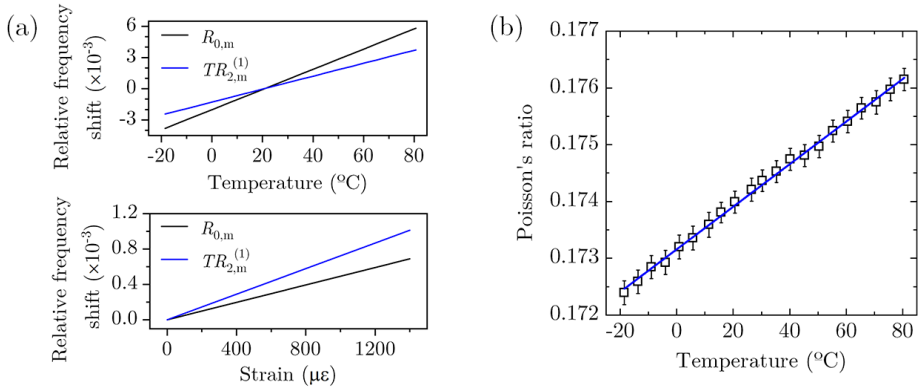

Figure 1. (a) Temperature and strain dependence of $R_{0,m}$ modes and $TR_{2,m}$ modes in an optical fiber. (b). Poisson's ratio of the optical fiber at different temperatures.

[1] A. S. Biryukov, M. E. Sukharev, and E. M. Dianov, *Quantum Electronics* **32**, 765 (2002).
[2] L. A. Sánchez, A. Díez, J. L. Cruz, and M. V. Andrés, *Optics Express* **30**, 14384 (2022).
[3] L. A. Sánchez, A. Díez, J. L. Cruz, and M. V. Andrés, *Optics Express* **30**, 42 (2022).

Acknowledgements: This work was supported by European Regional Development Fund (PDI2019-104276RB-I00); European Commission (H2020-MSCARISE-2019-872049); Generalitat Valenciana (IDIFEDER/2020/064, PROMETEO/2019/048); Ministerio de Ciencia, Innovación y Universidades (PDI2019-104276RB-I00).

Two lines of space reserved to include
codes of the symposium and of this communication

Collinear optical vortices with tailored topological charge generated by angular momentum transfer

Ignacio Lopez-Quintas[1,*], Warein Holgado[1], Rokas Drevinskas[2], Peter G. Kazansky[2], Íñigo J. Sola[1], Benjamín Alonso[1]

[1]*Grupo de Aplicaciones del Láser y Fotónica (ALF). Deparatmento de Física Aplicada, Universidad de Salamanca, Spain.*
[2]*Optoelectronics Research Centre, University of Southampton, United Kingdom.*

*e-mail: ilopezquintas@usal.es

Special light beams exhibiting a structured field and carrying orbital angular momentum (OAM) appear as interesting tools in different fields such as particle manipulation, telecommunications or in several areas of light-matter interaction, including materials processing and nonlinear optics, among others. The coupling of spatially varying linear polarization fields (*i.e.,* radial or azimuthal) with spin and orbital angular momenta can be exploited to obtain optical vortices exhibiting different topological charges [1]. We propose a versatile in-line method suitable to obtain collinear optical vortices from focused or collimated beams, being continuous wave or pulsed. We consider a radial input mode of the form $R_m^{l_0}$ where l_0 and m denote the corresponding OAM and polarization azimuthal index respectively (m defined as the number of times that the orientation of the local linear polarization distribution is rotating 2π radians for a variation of 2π radians in the azimuthal coordinate) and demonstrate theoretically that there is a different OAM transfer to the final vortices depending on the m value of the input beam. Numerical simulations of the output vortices agree with the theoretical predictions, which are further confirmed by experimental measurements (see Fig. 1).

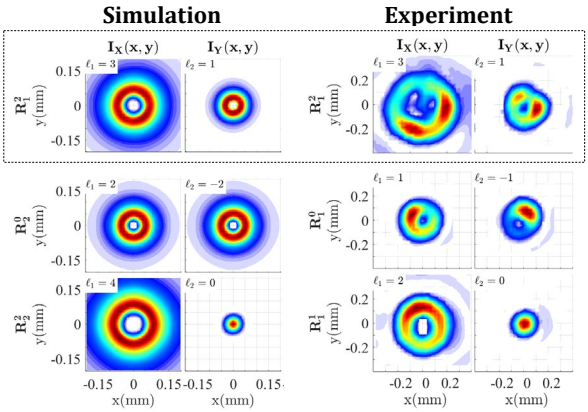

Figure 1. Representation of the x and y components of the spatial intensity profiles in focused beams for several simulated and experimental vortices [1]. For the R_1^2 case (top panels) a direct comparison between the simulated and experimental results can be made, illustrating the good agreement.

For the experiments, we used femtosecond laser pulses and combinations of special structured waveplates (s-waveplates) with standard retarders to generate radial modes with different additional OAMs that were used as input to produce the final optical vortices. Characterization of the obtained vortices was performed by a combination of the STARFISH technique and in-line interferometry [2-4]. Due to the perpendicular linear polarization of the obtained vortices, these can be separated and individually manipulated in potential applications. Thanks to its simplicity, the proposed method has been successfully applied for the generation of time varying optical vortices characterized by a novel technique [5].

[1] I. Lopez-Quintas, W. Holgado, R. Drevinskas, P. G. Kazansky, I. J. Sola, B. Alonso, *Journal of Optics* **22**, 095402 (2020).
[2] B. Alonso, I. J. Sola, O. Varela, J. Hernandez-Toro, C. Mendez, J. San Roman, A. Zaïr, L. Roso, *Journal of the Optical Society of America* **27**, 933 (2010).
[3] B. Alonso, I. J. Sola, *IEEE Journal of Selected Topics in Quantum Electronics* **25**, 8900307 (2019).
[4] B. Alonso, I. Lopez-Quintas, W. Holgado, R. Drevinskas, P. G. Kazansky, C. Hernández-García, I. J. Sola, *Communication Physics* **3**, 151 (2020).
[5] M. López-Ripa, Í. J. Sola, B. Alonso, *Photonics Research* **10**, 922 (2022).

Light polarisation under evanescent coupling in exciton-polariton couplers

Juan Lizarraga[1,*], A. Yulin[2], J. Beierlein[3], S. Klembt[3], S. Höfling[3], C. Antón-Solanas[1], M. D. Martín[1], L. Viña[1,4]

[1]*Dept. Física de Materiales & Inst. N. Cabrera, Univ. Autónoma, Madrid 28049, Spain.* [2]*Faculty of Physics and Engineering ITMO University St. Petersburg 197101, Russia.* [3]*Technische Physik, Universität Würzburg, Am Hubland, D-97074 Würzburg, Germany.* [4]*Instituto de Física de la Materia Condensada, Universidad Autónoma, Madrid 28049, Spain*

*e-mail: juan.lizarraga@estudiante.uam.es

Exciton polaritons are solid-state quasi-particles resulting from the strong interaction of light and matter. They constitute a quantum fluid possessing properties that bridge the best characteristics of light (low effective mass, extended spatial and temporal coherence) and matter (Coulomb interactions, magnetic response). A lateral patterning in semiconductor microcavities (via controlled dry etching) allows to arrange polaritons in versatile geometries, providing fundamental and application-oriented results, from topological simulators [1], to one-dimensional waveguides with a large list of functionalities [2].

Pushing forward our research on waveguided polaritons, our recent studies have focused on a polariton device consisting of two coupled one-dimensional waveguides (see sample image in Fig. 1a), where polaritons, injected in one of the input terminals (Fig. 1a-[I]), display Josephson-like oscillations between the two coupled waveguides (Fig. 1a-[II]) [3]. The resulting polariton splitting ratio in the output terminals (Fig. 1a-[III]) can be controlled via different parameters (e.g. laser pump power, and length of coupling region), and interestingly, our results show that the polariton population in each output waveguide is polarisation dependent and display polarisation beatings [4].

In this work, we study the degree of linear polarisation (DLP) and its propagation characteristics at the output terminals, after experiencing Josephson-like interactions through a long (50 µm) coupling region (see Fig. 1b where the DLP is evaluated in the vertical (*V*) and horizontal (*H*) polarisation basis). The DLP map shows orthogonally polarised polaritons in the up/down output terminals (blue/red color, respectively). We extend our analysis to quantitatively compare the polariton populations in the up/down output terminals as a function of the linear polarisation orientation of the polariton emission, see Fig. 1c. We find that the polariton populations in both terminals reach their maxima around the diagonal polarisations (*D*= diagonal, *A* = antidiagonal), since these constitute the polarisation eigenstates for polariton propagation. Furthermore, we also observe a small phase difference between these maxima and the exact D/A azimuths, which is probably related to certain experimental parameters such as Josephson-like coupling strength, pumping power or length of the coupling region.

This polariton coupler constitutes a fundamental example of an all-optical solid-state device that controllably splits information (propagating polariton condensates) encoded in the polarisation degree of freedom. Further experiments under resonant excitation would allow to increase the degree of polariton coherence and, probably, harness more functionalities in such a device via interference.

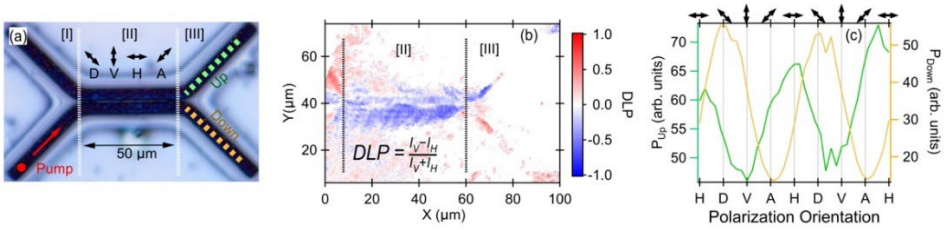

Figure 1. (a) Optical microscope image of a polariton coupler: [I] input terminals, (red circle indicates the pump laser), [II] coupling region, [III] output terminals (green/orange dotted lines: regions where the polariton populations are studied). Linear polarisations are labelled as A (anti-diagonal), V (vertical), H (horizontal) and D (diagonal). (b) Real space map of the DLP in the regions [II, III]. (c) Polariton populations in the up (green) and down (orange) output terminals as a function of the linear polarisation orientation. $P_{up/down}$ are obtained integrating the emission intensities in panel (a).

[1] P. St-Jean *et al.*, *Nature Photon* **11**, 651 (2017).
[2] M. Klaas *et al*., *Appl. Phys. Lett.* **114**, 061102 (2019).
[3] J. Beierlein *et al.*, *Phys. Rev. Lett.* **126**, 075302 (2021).
[4] E. Rozas *et al.*, *ACS Photonics* **8**, 2489 (2021).

Two lines of space reserved to include
codes of the symposium and of this communication

High-performance simulations of high-order harmonic generation based on artificial intelligence

Javier Serrano[1,*], Carlos Hernández-García[1]

[1] *Grupo de Investigación en Aplicaciones del Láser y Fotónica, Departamento de Física Aplicada, Universidad de Salamanca, Pl. La Merced s/n, Salamanca E-37008, Spain.*

*e-mail: fjaviersr@usal.es

Artificial intelligence is an emerging field that is being successfully used in a broad set of fields and applications, including physics. Thanks to the growing computing power provided by modern GPUs —and software libraries that allows to easily use these technologies—, artificial intelligence (and particularly deep learning) is becoming a powerful tool in ultrafast and nonlinear optics. For example, machine learning algorithms can predict the X-ray pulse properties of free electron lasers [1].

One of the fields in which artificial intelligence may provide powerful computing capabilities is in the simulation of high-order harmonic generation (HHG). HHG is a nonperturbative process in which high-order harmonics— extending up to the X-rays— result from the highly nonlinear interaction of an intense, infrared femtosecond laser pulse, with an atomic, molecular or solid target. The exact simulation of HHG requires a detailed evolution of the electronic wavepacket dynamics in the vicinity of each atom or molecule of the target, which is obtained through the resolution of the time-dependent Schrödinger equation (TDSE). Solving TDSE for single-atom HHG simulations using modern hardware is quite time consuming. However, a simulation that can be compared to experiments requires its macroscopic description, i.e. to account for the harmonic emission in all the atoms in the target. Thus, the macroscopic simulation would require to solve the TDSE 10^3 to 10^6 times, which makes the macroscopic simulation prohibitive. Our group has expertise in the development of microscopic and macroscopic approaches to simulate HHG in the most stringent situations [2, and citations therein]. Interestingly, it has been recently proposed to use deep neural networks to speed-up the microscopic TDSE calculation in HHG [3].

In this work we propose to apply artificial intelligence to macroscopic simulations of HHG. We create and train a neural network to infer single-atom HHG calculated through the TDSE (see Fig. 1), so macroscopic calculations can take advantage of this trained network to obtain experimentally comparable results of TDSE. This improvement will allow us not only to accelerate the macroscopic simulations of HHG, but to obtain for the first time TDSE-based macroscopic simulations of HHG, without the need of resorting to approximations like the Strong Field Approximation. As a consequence, studies of the macroscopic signature of effects that are not well reproduced in such approximations, like electronic correlations or the properties of low-order, perturbative harmonics, can be theoretically studied. In addition, we belive that artificial intelligence can set the path towards in-situ simulations that can guide future HHG experiments.

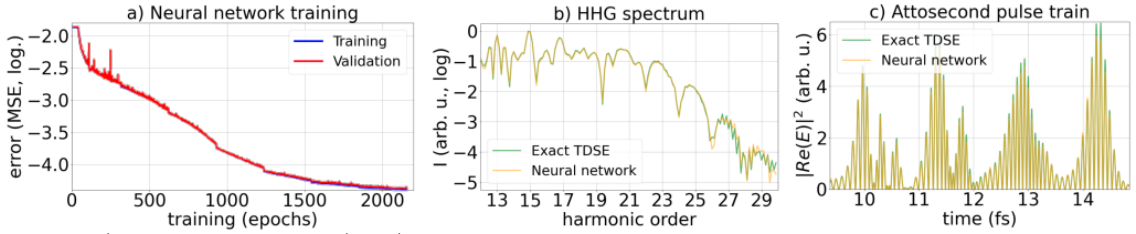

Figure 1. a) Evolution of the error (MSE) of the neural network during training with the TDSE. Sample single-atom results in the frequency (b) and time (c) domain using TDSE (green) and the neural network (orange).

[1] Sanchez-Gonzalez, A., Micaelli, P., et al. Accurate prediction of X-ray pulse properties from a free-electron laser using machine learning. *Nat Commun* **8**, 15461 (2017)

[2] Hernández-García, C., A. Pérez-Hernández, J., et al. High order harmonic propagation in gases within the Discrete Dipole Approximation, *Physical Review A* **82**, 033432 (2010)

[3] Lytova, M., Spanner, M. et al. Deep learning and high harmonic generation, *arXiv:2012.10328v2* (2021)

Acknowledgements: This work has been funded by the ERC Starting Grant ATTOSTRUCTURA, grant agreement No. 851201; Ministerio de Ciencia de Innovación y Universidades (PID2019-106910GB-I00, RYC-2017-22745); Junta de Castilla y León FEDER (SA287P18).

Efficient computation of azimuthal perturbation eigenpairs of vortex solitons

José R. Salgueiro*, Ángel Paredes, Humberto Michinel

Universidade de Vigo, E.E. Aeronáutica e do Espazo, Ourense 32004.

*e-mail: jrs@uvigo.es

Calculation of the perturbation eigenstates of non linear systems with angular momentum, i.e. those supporting vortex solitons, has proved to be problematic in the past. Although the eigenvalue problem is well defined and actually has been already solved for some different systems, its solution often requires from a big computational effort and long computation times, obtaining even sometimes erroneous results if the problem is not managed with care. Here we present a systematic method to get fast solutions which allow to know about the stability of the different stationary states of this kind of systems. We apply it to a system described by the cubic-quintic nonlinear Schrödinger equation for the sake of comparison, but it is applicable to other systems of the like.

The z-direction propagating vortex-like stationary states of such media come described by a function $\Psi(r,\phi,z) = \psi(r)\exp(il\phi)\exp(i\beta z)$, where $l = 1, 2, \ldots$ is the angular momentum, β is the propagation constant and $\psi(r)$ the r-dependent field envelope. This function fulfills the nonlinear Schödinger equation,

$$i\frac{\partial \Psi}{\partial z} = -\nabla^2\Psi - (|\Psi|^2 - |\Psi|^4)\Psi. \tag{1}$$

The stability of solutions can be studied by azimuthally perturbing them with small functions $F(r,z) = f(r,z)\exp[i(l+p)\phi]\exp[(\delta+i\beta)z]$ and $G(r,z) = g(r)\exp[i(l-p)\phi]\exp[(\delta^*+i\beta)z]$, where p is the order of the perturbation and δ the growth rate (real part). Replacing the perturbed state into the system equation (1) yields, after linearization, a pair of evolution equations for the perturbations F and G. These functions, together with the rate δ, were traditionally obtained by propagating these perturbed linearized equations until the perturbation fields F and G no longer change its shape and the growth rate stabilizes [1,2]. This is actually a version of the direct power method. Convergence is usually slow requiring from a long propagation distance and a long computation time, specially in cases for which the growth rate is close to zero (weak instability). In this case it is also necessary to increase the number of sampling points to get enough accuracy.

In order to improve the efficiency we chose to solve the problem changing the strategy. First, from replacement of the perturbed field into Eq. (1) it is obtained a generalized eigenvalue problem $\mathcal{A}(f|g^*)^T = (i\delta)\mathcal{B}(f|g^*)^T$, where $(i\delta)$ is the eigenvalue and matrices $\mathcal{A}$ and $\mathcal{B}$ are,

$$\mathcal{A} = \begin{pmatrix} \nabla_r^2 - \frac{(l+p)^2}{r^2} + Q & R \\ R & \nabla_r^2 - \frac{(l-p)^2}{r^2} + Q \end{pmatrix} \Bigg\| \mathcal{B} = \begin{pmatrix} -I & 0 \\ 0 & I \end{pmatrix}$$

being I a identity subblock matrix, $\nabla_r^2 \equiv \partial_r^2 + (1/r)\partial_r$, $Q = -\beta + (2n_2 - 3n_4\psi^2)\psi^2$ and $R = (n_2 - 2n_4\psi^2)\psi^2$. Matrix $\mathcal{A}$ is real but non-symmetric and so it may contain complex eigenvalues. Actually, those in the form of complex conjugate pairs are the interesting ones as the imaginary part accounts for the real part of δ which is the growth rate of the perturbation. Finding no complex eigenvalues is then an indication of the system stability.

The eigenvalue problem is solved using a combined method to improve efficiency. First, a direct eigenvalue solver (as for instance the QZ algorithm) is used with a coarse number of points (few hundreds of samples) in order to estimate the eigenvalues and select the interesting ones (complex conjugate pairs if any). Then, this estimation is refined to a much finer sampling using the inverse power method. Following this strategy we were able to compute solutions with 5×10^4 samples without too much effort. This technique allowed to reproduce the results for the stability of bright vortex solitons [2] as well as to determine the stability of the dark solitons supported by a cubic quintic model. The method is, however, useful for more general nonlinear systems supporting vortex solitons.

[1] Soto-Crespo, J. M., Heatley, D. R., Wright, E. M., Akhmediev, N. N., *Phys. Rev. A* **44**, 636 (1991).
[2] Michinel, H., Salgueiro, J. R., Paz-Alonso, M. J.,*Phys. Rev. E* **70**, 066605 (2004).

Acknowledgements: We thank the support of MCIN of Spain through the project PID2020-118613GB-I00, as well as Xunta de Galicia (grant ED431B 2021/22).

Two lines of space reserved to include
codes of the symposium and of this communication

Quantum liquids and droplets with low-energy interactions in one dimension

I. Morera[1], B. Juliá-Díaz[1], **M. Valiente**[2,*]

[1] *Departament de Física Quàntica i Astrofísica, Facultat de Física, Universitat de Barcelona, Barcelona, Spain.* [2] *Departamento de Física, Universidad de La Laguna, Tenerife, Spain.*

*e-mail: mvalient@ull.edu.es

We consider interacting one-dimensional bosons in the universal low-energy regime. The interactions consist of a combination of attractive and repulsive parts that can stabilize quantum gases, droplets and liquids. In particular, we study the role of effective three-body repulsion, in systems with weak attractive pairwise interactions. Its low-energy description is often argued to be equivalent to a model including only two-body interactions with non-zero range. Here, we show that, at zero temperature, the equations of state in both theories agree quantitatively at low densities for overall repulsion, in the gas phase, as can be inferred from the S-matrix formulation of statistical mechanics. However, this agreement is absent in the attractive regime, where universality only occurs in the long-distance properties of quantum droplets. We develop analytical tools to investigate the properties of the theory, and obtain astounding agreement with exact numerical calculations using the density-matrix renormalization group. [1]

[1] I. Morera, B. Juliá-Díaz and M. Valiente, arXiv:2103.16499 (2021).

Two lines of space reserved to include
codes of the symposium and of this communication

Fiber-based biphoton spectroscopy

I. Pérez Pérez[1,*], M. Afsharnia[1], M. Weißflog[1], S. Saravi[1], T. Pertsch[1,2], F. Setzpfandt[1,2]

[1]*Institute of Applied Physics, Abbe Center of Photonics, Friedrich-Schiller-University Jena, Albert-Einstein-Str. 15, 07745 Jena, Germany.*

[2]*Fraunhofer Institute for Applied Optics and Precision Engineering, Albert-Einstein-Str. 15, 07745 Jena, Germany.*

*e-mail: inmaculada.perez.perez@uni-jena.de

Entangled photon pair sources are of great interest thanks to their many potential applications in quantum technologies. Due to their potential, big efforts are put into developing sources with specific characteristics. One of the challenges faced in this context is the characterization of the resulting photon pairs.

In this project, we implement a simple method to estimate the wavelengths of spectrally correlated photon pairs by means of a dispersive medium. This can be especially useful for setups where direct spectroscopy measurements are not possible.

This method has been tested for photon pairs produced with different sources: one generated by Spontaneous Parametric Down Conversion (SPDC) and the other by Spontaneous Four Wave Mixing (SFWM). The photons are each coupled into a long single-mode optical fiber and eventually reach a Single Photon Detector (SPD). The difference between their times of arrival is measured and used to determine their wavelengths based on the corresponding energy conservation law and the dispersive nature of the fibers, which act as a delay line.

The calculated wavelengths show a good agreement with our reference values, with percent errors under 5%. This study was performed assuming steady conditions where potential disturbances such as vibrations or temperature gradients were not considered. Additionally, we observed a high sensitivity to the length of the dispersive elements. Solutions to this problem are discussed in the poster.

Despite these limitations, our results suggest that this method can be implemented for future spectroscopy measurements of correlated photon pairs as long as the corresponding energy conservation law and the dispersion character of the fibers are known.